Polarforschung 82 (1), 1–18, 2012

Advances of Sea-Ice Observations since ARCTIC 91*

by Wolfgang Dierking[1] and Christian Haas[2]

Abstract : One of the first systematic sea ice studies in the central Arctic was carried out in 1991 during the International Arctic Ocean Expedition ARCTIC 91. The work program included in-situ measurements of physical sea-ice properties, and ground-based radar measurements in conjunction with the launch of the European Remote Sensing satellite ERS-1. Based on results and experiences made during this expedition, new measurement techniques were developed in the following years, in particular for the retrieval of sea-ice thickness. They were successfully tested and applied on several expeditions into the pack ice of the Arctic and Antarctic. Satellite instrument technology as well as the methods for analysing space-borne sea-ice observations have made large progress. Now, more than twenty years later, the annual Arctic summer sea-ice minimum extent has decreased dramatically, and the collected knowledge about sea-ice properties and interaction mechanisms between ocean, sea ice, and atmosphere is a key ingredient in explaining recent sea-ice cover variations and their impact on regional and global climate. In this paper, the authors pick up examples how sea-ice observation technology advanced during the past twenty years, thereby focusing on topics, which have largely been initiated during the ARCTIC 91 expedition.

Zusammenfassung: Eine der ersten systematischen Untersuchungen des Meereises in der zentralen Arktis wurde 1991 während der Internationalen Nordpolarmeer-Expedition (ARCTIC 91) durchgeführt. Das Arbeitsprogramm beinhaltete in-situ Messungen von physikalischen Eigenschaften des Meereises sowie bodengebundene Radarmessungen im Zusammenhang mit dem Start des europäischen Fernerkundungssatelliten ERS-1. Auf Grundlage der auf dieser Expedition gewonnenen Ergebnisse und Erfahrungen wurden in den folgenden Jahren neue Messtechniken entwickelt, insbesondere für die Ermittlung der Meereisdicke. Diese Techniken wurden erfolgreich getestet und auf zahlreichen Expeditionen in das Packeis der Arktis und Antarktis angewendet. Auch die Technologie von Satelliteninstrumenten und die Methoden der Satellitendatenauswertung haben große Fortschritte gemacht. Mehr als zwanzig Jahre nach ARCTIC 91 nimmt das Sommerminimum der Meereisausdehnung dramatisch ab, und das gesammelte Wissen über die Eigenschaften des Meereises und die Wechselwirkung zwischen Ozean, Eis, und Atmosphäre ist eine wichtige Voraussetzung zur Erklärung von gegenwärtigen Variationen der Meereisbedeckung und deren Einfluss auf das regionale und globale Klima. In diesem Artikel zeigen die Autoren anhand von Beispielen, wie sich die Technologien zur Beobachtung des Meereises in den letzten 20 Jahren weiterentwickelt haben. Dabei konzentrieren sie sich auf Themenbereiche, die zu einem großen Teil auf der ARCTIC 91-Expedition angestoßen wurden.

INTRODUCTION

The expedition ARCTIC 91 (ARK-VIII/3, 1991) of the German research vessel "Polarstern" and the Swedish icebreaker "Oden" into the pack ice of the central Arctic was in many respects special for the participating sea-ice researchers from Germany, Sweden, and Finland. The joint ship operations facilitated movements in the ice considerably. Fruitful cooperations between scientists on board both vessels were established. The European Remote Sensing (ERS-1) satellite had been launched on 17 July 1991, i.e., only a few days before "Polarstern" headed for the Arctic Ocean on 01 August. And finally, plans about developing and applying new technologies for the measurements of sea-ice thickness took shape in the heads of the participating specialists who until then almost solely had used ice drills. As it turned out, the ARCTIC 91 expedition strongly influenced sea-ice research at the Alfred Wegener Institute (AWI). In this article, a brief overview is given on how different research activities, including field-work on the ice and data acquisitions from helicopters, aircrafts, and satellites over the ice, evolved over the past two decades. The 1991-expedtion is taken as a starting point for the (necessarily) brief (and therefore incomplete) historic journey through the evolution of sea-ice observation technology since then. Unfortunately it is not possible to mention all the numerous interesting and exciting results that were obtained during the last two decades. We focused on topics with a strong link to the sea ice and remote sensing program of the ARCTIC 91 expedition and to the recent changes of sea-ice thickness observed in the Arctic. Only now and then the look will be directed also to the Antarctic and the Baltic Sea. Readers interested in a more comprehensive overview of topics related to physics and observations of sea ice are referred to the textbooks by WADHAMS (2000) and LUBIN & MASSOM (2006) and the studies cited therein.

First, we present an introduction to the atmosphere – sea-ice – ocean system and its current state, followed by fundamentals of remote sensing methods. These two sections provide the reader with some background knowledge. Then we touch upon the situation in Arctic sea-ice research and remote sensing in the early 90s and pick up examples of corresponding results from the ARCTIC 91 expedition. In the subsequent sections we deal with the development of ice thickness measurement technology and the knowledge about variations and trends of sea-ice thickness gained during the past twenty years. This part is followed by a presentation of advances in sea-ice observations by space-borne imaging radar from the early 90s until present. The emphasis is on the increasing technological flexibility of imaging radar systems, the benefit of combining satellite, airborne and ground-based measurements, on ice-type classification, on the retrieval of ice surface characteristics from radar images, and on the changes in the appearance of sea ice in radar images during the melt season. Finally, we take a look into the future of sea-ice research and remote sensing.

THE ATMOSPHERE – SEA ICE – OCEAN SYSTEM AND ITS CURRENT STATE

Large areas of the ocean's surface are covered by ice wherein the ice extent is varying considerably over the seasons. In the Arctic, it increases from 7 to 14 million km^2 from summer to winter, for the Antarctic the corresponding numbers are 4 and

---

* Extended version of an oral presentation at the "20 year North Pole anniversary symposium" 7 September 2011 at IfM-GEOMAR, Kiel.

[1] Alfred Wegener Institute for Polar and Marine Research, Bussestraße 24, D-27570 Bremerhaven, Germany; <wolfgang.dierking@awi.de>

[2] University of Alberta, Depts. Earth & Atmospheric Sciences and Geophysics, Edmonton, Alberta, T6G 2E3, Canada; <chaas@ualberta.ca>

Manuscript received 06 March 2012, accepted in revised form 19 July 2012.

20 million km^2, respectively. For comparison, the USA cover an area of 9.6 million km^2, Russia's extent is 17.1 million km^2.

Why should one be interested in sea ice? In fact, it induces or influences a number of processes that have direct or indirect impact on Earth's climate. From the ice surface, a much larger fraction of the incoming solar radiation is reflected back into space than from the surface of the open ocean. This mechanism affects the ocean and air temperatures, which would be higher without any ice coverage in the Polar Regions. Sea ice forms a barrier between the atmosphere above and the ocean below, i.e., it reduces or even stops the exchange of heat, moisture and matter. It also changes the transfer of momentum between ocean and atmosphere. The energy transfer from wind to waves is replaced by a near-surface air flow influenced by an irregular mixture of level ice, open water leads, edges of single ice floes, and ice blocks piled up in ridges (Fig. 1).

When sea ice forms, the salt contained in the water accumulates in small liquid-filled pores between the ice crystals. This brine is expelled into the water layer beneath the ice. As the upper water layer gains weight due to the inflow of dense brine, it may eventually become heavier than the water mass below and start to sink down. In many cases, such processes remain local effects, but if the areas of growing ice are large and special conditions are met (e.g., a weak density stratification of the water column below the ice), the brine rejection induces kilometre-scale convection in the ocean, which even affects the global ocean circulation.

Long-term changes of the sea-ice cover state are regarded as an indicator of broader climate change such as global warming. When viewed from space, the ice cover is visible over the entire Arctic Ocean and adjacent ocean basins. Variations of the ice extent can be determined on different temporal scales. A sequence of daily images collected over a whole year

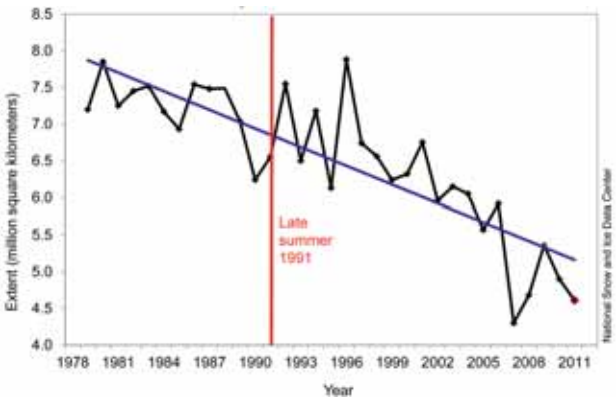

Fig. 2: Average monthly Arctic sea ice extent in September for the years 1979 to 2011 derived from satellite observations. The vertical red line marks the timing of the ARCTIC 91 expedition.

Abb. 2: Monatsmittel der arktischen Meereisausdehnung für September über die Jahre von 1979 bis 2011, abgeleitet aus Satellitendaten. Die senkrechte rote Linie markiert den Zeitpunkt der ARCTIC 91-Expedition.

reflects the increase of ice extent from summer to winter and the succeeding decrease from winter to summer. For climate research, it is more interesting to compare the ice extent measured on a fixed date for a number of years. In Figure 2, a curve resulting from this approach is shown. Here, the date of the minimum extent during summer was taken as the annual reference point. It shows large variations from year to year. But more importantly, it reveals a significant decrease of ice extent over the last decades. This trend was not obvious in 1991, with corresponding data available only for a little more than one decade. The curve represents the total, Arctic-wide sea-ice extent. Since this is an area of 7 million km^2, a closer look at local and regional ice conditions is useful. Figure 3 shows maps of sea-ice concentration gathered at the timing of the summer sea-ice minimum in the years from 2005 to 2010. At some locations, the spatial distribution of the ice cover and of the belts of equal ice concentration differs from year to year. One example is the Beaufort Sea north of Canada. At other locations, ice conditions appear to be more stable, for example north of Greenland. Such image sequences are useful when it comes to explaining the observed decrease of the Arctic sea-ice cover. However, they cannot be employed as isolated information. It is important to collect all relevant data on atmospheric and oceanic conditions. Different hypotheses are then examined with computer

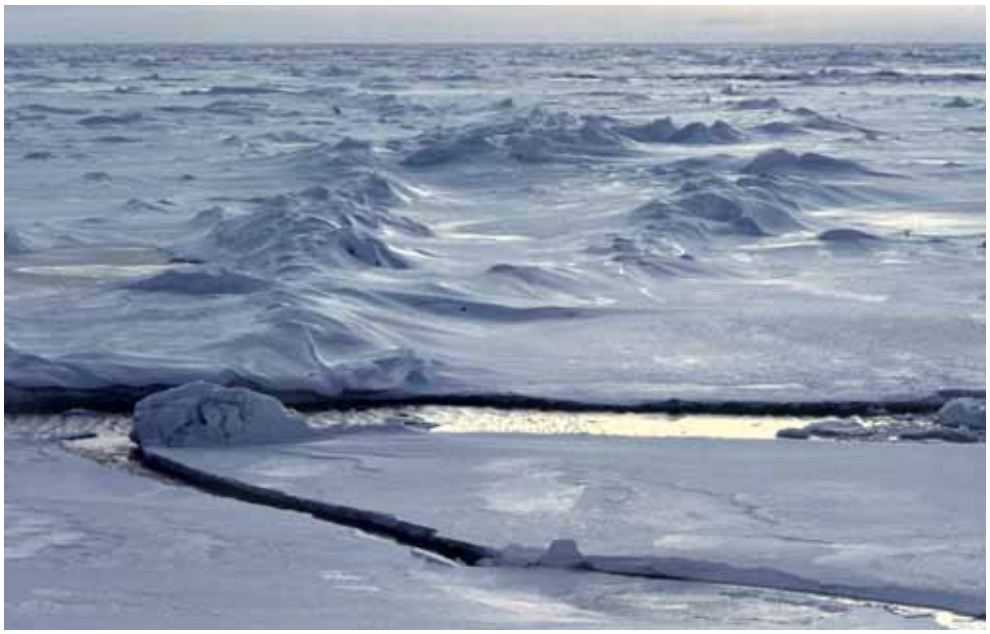

Fig. 1: Sea-ice floes in the Arctic, with ice ridges and open water leads (Photo: W. Dierking).

Abb. 1: Eisrücken-bedeckte Meereisschollen in der Arktis durch Wasserrinnen voneinander getrennt (Foto: W. Dierking).

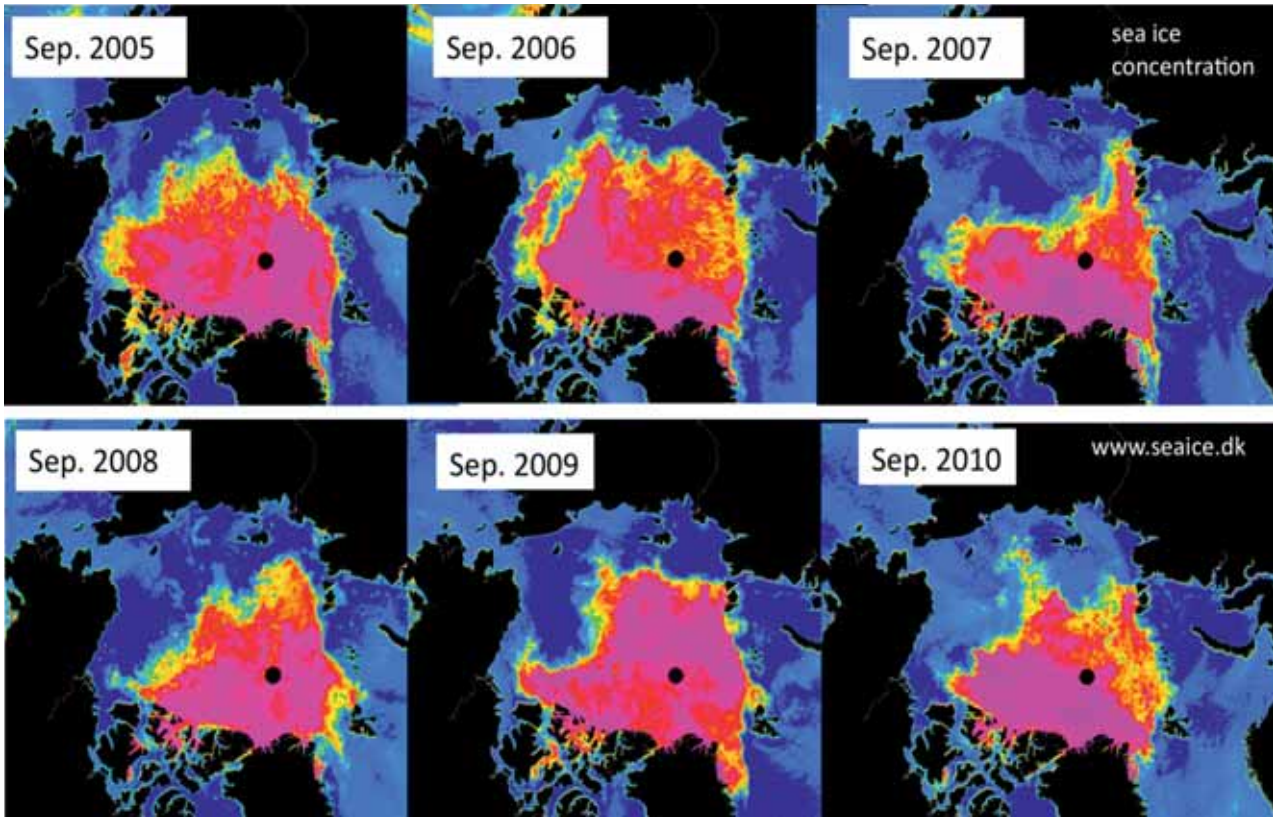

Fig. 3: Arctic sea-ice coverage at the time of the annual summer minimum for different years. The colours indicate the magnitude of sea-ice concentration (i.e. the fraction of a unit area on the ocean surface covered by ice). Blue is open water, green and yellow indicate low to moderate ice concentrations, and red and violet high concentration up to a closed ice cover. Source: http://seaice.dk.

Abb. 3: Meereisbedeckung der Arktis zum Zeitpunkt des jährlichen Sommerminimums für verschiedene Jahre. Die Farben zeigen das Werteintervall der Eiskonzentration (d.h. des vom Eis bedeckten Flächenanteils eines Meeresgebietes). Blau bedeutet offenes Wasser, grün und gelb sind geringe und mittlere Konzentrationen, rot und violett bedeuten hohe Konzentrationen bis zu einer geschlossenen Eisdecke. Quelle: http://seaice.dk.

simulations that are based on physical models. Such models describe the interactions between atmosphere, sea ice, and ocean and use measured meteorological and ocean data as input.

The absolute minimum in Arctic sea-ice extent hitherto was observed in summer 2007. Scientists (e.g., STROEVE & SERREZE 2008) named as key factors:
- ice pack thinning in preceding years,
- an unusual pattern of atmospheric circulation in 2007, during which persistent southerly winds gave rise to higher temperatures and ice transport away from the Siberian coast and Beaufort Sea, and
- predominantly clear skies fostering strong melt.

What can be expected for the future? Any answer to this question is not indisputable. Climate model projections indicate that the Arctic may be ice-free during summers already in the late 2020s (WANG & OVERLAND 2009). It is concluded that an anthropogenic influence on the most extreme negative trends in sea-ice extent is evident, but the effect of the natural variability can be strong on timescales between two and ten years (KAY et al. 2011). The perennial ice fraction in the Arctic reveals large rates of decline, which is in agreement with the observation of a decrease in the average ice thickness (COMISO 2012).

At this point it is interesting to also have a closer look on the Antarctic. Overall, there has been a slight increase in the maximum Antarctic sea-ice extent – but there are significant regional differences. At the western side of the Antarctic Peninsula, in particular in the Bellingshausen Sea, an increase in average winter air temperature, a warming of the ocean surface and a change to more northerly winds have been observed recently, which cause a decline of the sea-ice covered area. In the Weddell and Ross seas, both the sea-ice extent and the length of the sea-ice season increase. In the Ross Sea, for example, this is attributed to changes in regional atmospheric circulation patterns. Sea-ice researchers are hence intensively focusing on the changes in the large-scale circulation patterns around Antarctica and their impact on the sea-ice cover (TURNER et al. 2009).

SEA ICE REMOTE SENSING

If one considers the huge areal extent of the Polar Regions and the logistic difficulties to access this partly hostile environment, it becomes evident why field measurements from those regions are spatially and temporally sparse. Hence, observations from space are extremely useful for polar research. But how can such data be applied in a meaningful way, considering that the measurement devices are flown hundreds of

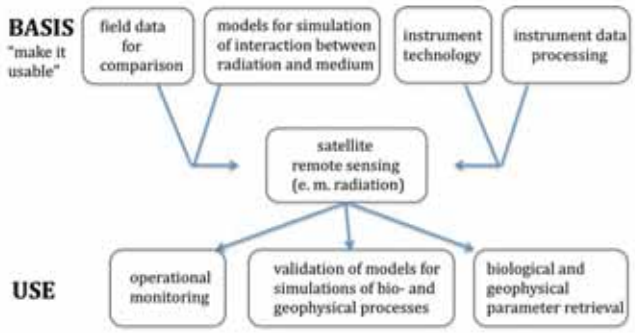

Fig. 4: The network of research disciplines around satellite remote sensing.

Abb. 4: Das Netzwerk von Forschungsdisziplinen, in dem die Fernerkundung eingebettet ist.

kilometres above the ice surface? In case of so-called passive instruments they measure the intensity of sunlight reflections or of thermal emission from the Earth surface. Active devices, such as laser or radar, transmit an electromagnetic signal and measure the travel time of this signal on its path between the satellite and the Earth's surface and back, and the signal echo intensity. In special instrument configurations, in which two and more signal channels are available, the phase differences between signals are also recorded. One of the major tasks of specialists working in the field of remote sensing is to develop methods by which a parameter of interest, for example sea-ice extent or concentration, can be retrieved from the directly measured quantities, for example from the brightness temperature. The latter depends on the physical temperature of an object and its emissivity, i.e., its "ability" to emit energy by radiation.

A major problem for remote sensing is that the Polar Regions are shrouded in clouds and darkness over long periods of the year. Hence, sensors measuring sunlight reflections or thermal infrared emission are only of limited use for sea ice and ocean research. A solution to this problem are instruments working with microwaves, i.e., with electromagnetic radiation in the wavelength range from 1 mm to 1 m, corresponding to frequencies between 300 and 0.3 GHz. Microwave sensors can see through clouds and are not affected by light conditions. However, scientist first had to learn how microwave radiation interacts with the medium "sea ice". Questions that had to be addressed were, for example, how one can explain the appearance of sea ice in radar images, or which frequency ranges reveal the largest emissivity contrasts between open water and different types of sea ice?

The successful use of remote sensing technologies for providing the information that is needed by sea-ice specialists and in other research disciplines requires the consideration of various aspects that are important for data interpretation and analysis (Fig. 4). The understanding on how sea-ice properties influence the emission, absorption, and scattering of microwave radiation has been developed on the basis of theoretical models. For such models, the results of field measurements are a mandatory input. How is sea ice structured? What do typical salinity and temperature profiles from the ice surface to the ice – water interface look like? How rough is the ice surface? How many air bubbles are found in the ice, how large are they, and which shape do they have? These are a few questions to which field measurements give answers. The questions arise from our fundamental knowledge of various processes that occur while an electromagnetic wave is propagating in a medium. For example, the incoming wave is partly reflected at the ice surface according to Snell's Law and partly scattered in all directions, dependent on the surface roughness. Also air bubbles in the ice scatter the electromagnetic waves. Some of the wave energy is absorbed, and the magnitude of absorption depends on ice salinity and temperature. The sea-ice model used for simulating the microwave signal measured by the satellite sensor is often a simplification of the real ice conditions. For example, vertical profiles of continuously changing densities and salinities are replaced by thin layers with constant physical properties, or air bubbles of arbitrary shape are approximated by spheres or ellipsoids. Vertical and lateral variations of physical sea-ice properties occur on different spatial and temporal scales and can in many cases only be quantified inadequately. For practical purposes, the algorithms for simulating different scattering mechanisms often need to be computationally efficient, which means that suitable approximations are employed.

Two other important aspects are to be considered when extracting information from remote sensing data, that is the instrument technology, and closely related to it the processing of the raw instrument data. Obviously, different factors such as spatial resolution, areal coverage, or the noise level of the instrument affect the information extraction. As part of data processing, various signal filters and algorithms can be used. Filters are applied, for example, to suppress inherent instrument artefacts. A large number of algorithms exist for information enhancement, data segmentation, data classification, and other tasks.

Remote sensing data are used mainly for operational services, but also for supporting studies on sea-ice properties, kinematics, and dynamics. Operational sea-ice monitoring has an immediate economical and social impact. Ice services in different countries have to provide local and regional-scale sea-ice charts and forecasting of ice conditions for seasonally or perennially ice-covered waters in support of marine transport and offshore operations. In sea-ice research, various data products derived from satellite measurements are a valuable basis for assessments on how realistically sea-ice conditions and their changes are reproduced by computer simulations of ocean – ice – atmosphere interactions. The closer such models simulate recent ice conditions dependent on various meteorological and oceanic input parameters, the more useful they are assumed to be for predictions of future sea-ice state.

As already mentioned above, one of the central tasks of remote sensing specialists is the development of retrieval algorithms or interpretation strategies, which link the satellite data to the actual ice conditions. In operational sea-ice mapping, for example, trained analysts generate sea-ice charts using optical and radar images from satellite instruments together with observations from airplanes, helicopters and ships. Thereby they may be supported by the results of computer-based analyses of sea-ice conditions such as ice extent, concentration, drift, thickness, degree of deformation, or occurrence of different ice types. The situation is similar in more scientifically motivated studies. In the latter case, spatial and temporal

scales of observations as well as the ice parameters of major interests may be different. Examples are the Arctic- or Antarctic-wide timing of melt-onset and freeze-up and the regional melt pond coverage.

SEA ICE MEASUREMENTS IN THE CENTRAL ARCTIC PRIOR TO 1991

Before ARCTIC 91, only few projects had systematically studied sea-ice properties in the Central Arctic Ocean. Knowledge about sea ice in that region until then was mainly based on:

- Nansen's "Fram" drift 1893-1896 (NANSEN 1897),
- Russian activities related to the "Sever" expeditions of airborne Arctic surveillance when measurements were performed during aircraft landings on ice floes or during the drift of North Pole Research Stations since 1937 (e.g., ROMANOV 1995, FROLOV et al. 2005),
- US and UK military nuclear submarine cruises, which carried upward-looking sonars for the measurement of sea-ice thickness and since 1958 occasionally surfaced at the North Pole (e.g., BOURKE & GARRET 1987).

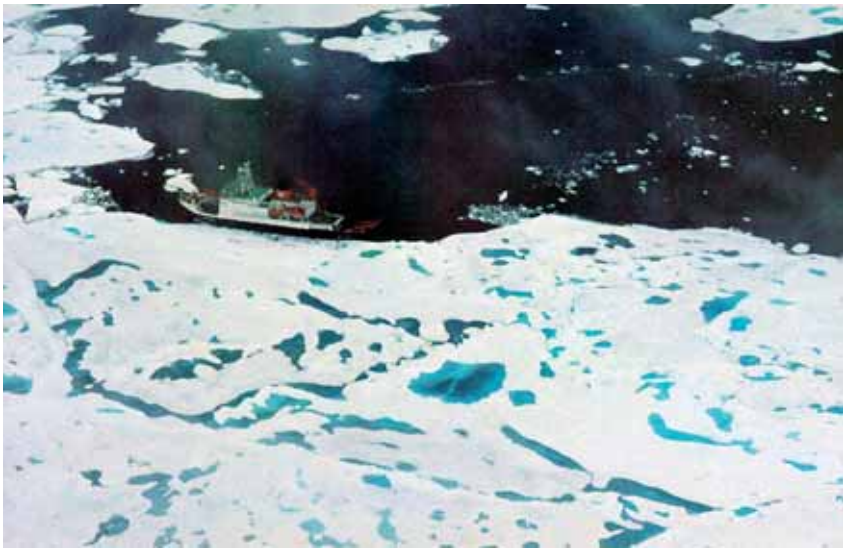

Fig. 6: Melt ponds on the sea ice in the central Arctic (Photo: W. Dierking).

Abb. 6: Mit Schmelztümpeln überdecktes Meereis in der zentralen Arktis (Foto: W. Dierking).

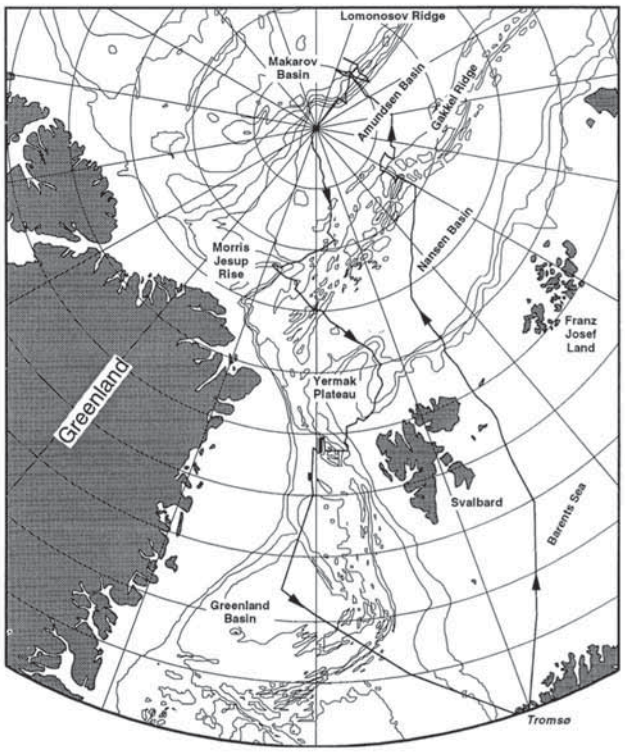

Fig. 5: Cruise track of RV "Polarstern" during Leg ARK-VIII/3 (ARCTIC 91), August – September 1991. Source: FÜTTERER 1992.

Abb. 5: Route von FS "Polarstern" im Sommer 1991 während des Fahrtabschnitts ARK VIII/3 (ARCTIC 91). Quelle: FÜTTERER 1992.

A number of scientific ice observations were made during the British Trans-Arctic Expedition in 1968/69 crossing the North Pole (KOERNER 1973), and significant studies were carried out in the Beaufort Sea during the US-Canadian Arctic Ice Dynamics Joint Experiment in the 1970s (AIDJEX, e.g, UNTERSTEINER et al. 2007). A detailed overview of the studies carried out prior to 1991 and of the results achieved until then are beyond the scope of this paper. At the beginning of the 1990s, comparatively little was known about structure, composition, and properties of Arctic multi-year ice (EICKEN et al. 1995). The knowledge on processes related to the Arctic melt season was in parts only marginal (EICKEN 1994). The potential of using satellite imaging radars for sea-ice observations was recognized in the late 1970s with the SEASAT mission (DIERKING & BUSCHE 2006) and through ice monitoring by Russian radar satellites since the early 1980s. Those research topics strongly influenced the activities of the sea ice and remote sensing teams that participated in the ARCTIC 91 expedition.

SEA-ICE MEASUREMENTS IN 1991

The ARCTIC 91 leg from Tromsø to the North Pole and back, which is addressed here, is shown in Figure 5. Preliminary results of the different measurement programs of the expedition are described in the cruise report (FÜTTERER 1992). In the following section, the sea-ice measurements and results are briefly summarized, as well as the data acquisitions carried out in conjunction with the remote sensing studies.

Actually, the ARCTIC 91 sea-ice sampling program was one of the first systematic sea-ice studies in the central Arctic (EICKEN et al. 1995). It included observations of ice conditions from the bridge of "Polarstern", helicopter observations of melt ponds on the ice surface (Fig. 6), ice-thickness measurements, and coring for physical, chemical, and biological analyses of the ice. The ice concentration along the ship's cruise (Fig. 5) in the pack ice was 91 ±13 %, and floe sizes

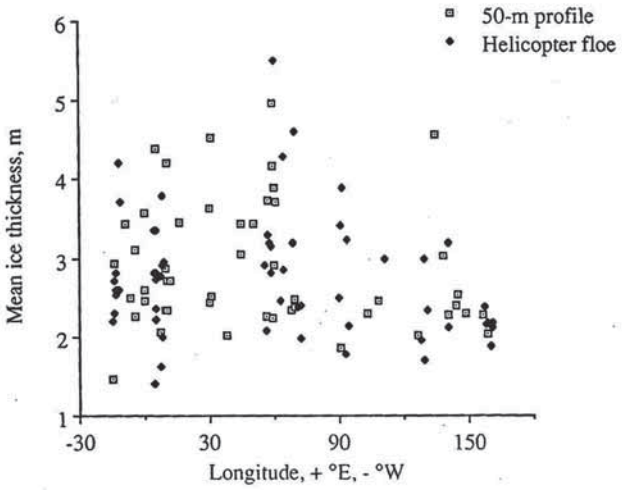

Fig. 7: Top: Drilling in a melt pond for ice thickness measurements (Photo: W. Dierking). Bottom: ice thickness measured during the cruise ARK-VIII/3 (ARCTIC 91) The ice thickness was either measured along 50 m long profiles or on different ice floes accessed by helicopter (from FÜTTERER 1992).

Abb. 7: Oben: Bohrung zur Ermittlung der Eisdicke unter einem Schmelzwassertümpel (Foto: W. Dierking). Unten: Während der Expedition ARCTIC 91 gemessene Eisdicken. Die Eisdicke wurde entweder entlang von 50 m langen Profilen oder auf verschiedenen Eisschollen ermittelt, die mit dem Hubschrauber angeflogen wurden (aus FÜTTERER 1992).

were frozen over by ice. More detailed analyses of these measurements are presented in EICKEN (1994) and EICKEN et al. (1995).

The remote sensing work on "Polarstern" was focused on collecting data for improving retrieval algorithms for sea-ice concentration and drift. To this end, Advanced Very High Resolution Radiometer (AVHRR) images with a horizontal resolution of 1 km were received on board (Fig. 8) (VIEHOFF 1990), and a line-scan camera was flown on the helicopter to obtain images with a horizontal resolution of 1-3 m (dependent on altitude) for comparison. The surface temperature was recorded with a ship-based radiometer and served as ground-truth for the AVHRR data. In addition, the ice surface topography was measured with a ground-based mechanical profilometer for studying the centimetre-scale roughness, and with an airborne laser altimeter mounted on a helicopter for detecting meter-scale undulations and determination of ice ridge statistics. The former was of interest for improving surface scattering models needed for simulating remote sensing data (see above), the latter served also as preparation for measurements in the Weddell Sea one year later (DIERKING 1995).

varied between hundreds of metres to few kilometres. In most cases, ridges and hummocks covered less than 5 % of the ice floe area, but at some locations, the corresponding value was as large as 30 %. Altogether 23 icebergs with a diameter of more than 100 m were sighted during the first half of the cruise. Level ice thickness data were collected in the vicinity of the ship along 50 m long profiles with a spacing of 5 m. In addition, thickness measurements were carried out on randomly chosen ice floes accessed by helicopter several kilometres away from the ship. For the first time ever, the pilots used GPS receivers to find their way back to the ship. The ice-thickness data are shown as a function of longitude in Figure 7. Ice cores were taken for on board analyses of ice texture, density, salinity, distribution and size of pores, and chlorophyll-a concentration. During helicopter flights, the areal fraction of melt ponds was recorded (Fig. 6). At some locations, ponds covered up to 50 % of the ice surface. At the end of August, almost all ponds

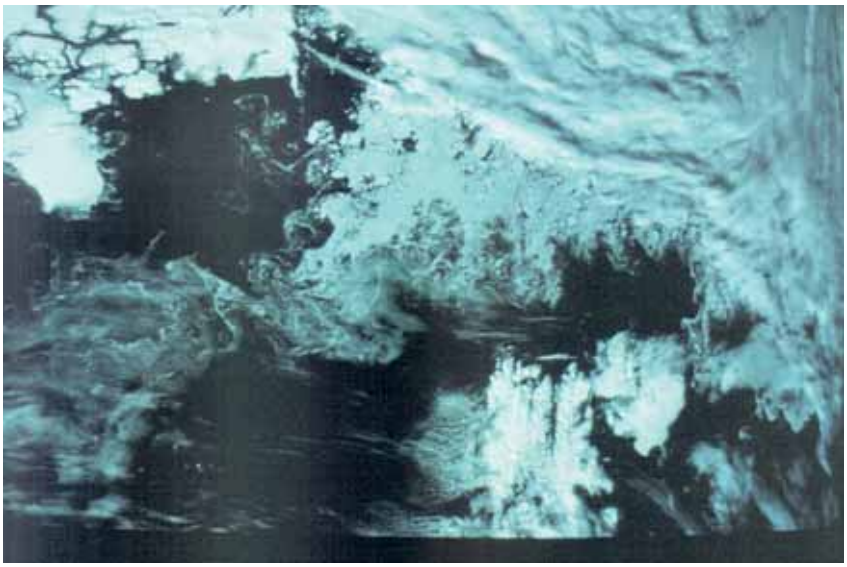

Fig. 8: AVHRR (Advanced Very High Resolution Radiometer) image (optical channel) received on RV "Polarstern". The image shows Fram Strait between the northeast coast of Greenland (upper left) and the northern part of Svalbard (lower right). In the centre of the image, the marginal sea ice zone is visible. To the north (upper right), the ice is hidden under clouds.

Abb. 8: Bild des Satelliteninstruments AVHRR (optischer Kanal), empfangen auf FS "Polarstern". Es zeigt die Framstraße zwischen der Nordostküste Grönlands (oben links) und dem nördlichen Teil Spitzbergens (unten rechts). In der Mitte des Bildes ist die Eisrandzone sichtbar. Im Norden (oben rechts) ist das Eis unter Wolken verborgen.

The data that were gathered by the remote sensing team on board "Oden" contributed significantly to a better understanding of the dominant interaction mechanism between radar waves and thick multi-year sea ice (CARLSTRÖM & ULANDER 1993). The team operated a ship-based radar system at the same frequency as the imaging radar on the ERS-1 satellite.

Concurrent to the radar data acquisitions from the ship, snow and ice properties were surveyed. The data acquisitions included snow depth along horizontal profiles, and snow density and wetness as a function of depth. The centimetre-scale ice surface roughness was measured using a laser profiler (Fig. 9). Ice density, temperature, and salinity were obtained from ice cores. Photographs were taken of the upper low-density ice layer, which were later used for determination of air bubble sizes.

The joint expedition of "Polarstern" and "Oden" emphasized the importance of ship cruises into sea-ice covered regions for detailed in-situ investigation of ice properties. The field program of "Polarstern" during ARCTIC 91 covered studies from biology, geology, and oceanography that all benefitted from the results of the sea-ice measurement program.

Fig. 9: Swedish laser system for measuring centimetre-scale roughness on the ice surface (Photo: W. Dierking).

Abb. 9: Das schwedische Lasersystem zum Messen der Eisrauigkeit im Zentimeterbereich (Foto W. Dierking).

OBSERVATIONS OF SEA-ICE THICKNESS SINCE 1991

Ground-based measurements of sea-ice thickness

The growing experience with ship operations in the central Arctic since 1991 made it possible to visit the region of the North Pole more regularly, offering new opportunities for more systematic work. Subsequently, significant sea-ice studies were performed during follow-up cruises of "Polarstern" in 1996, 1998, 2001, 2007, and 2011 (see below), and during Canadian, US, and Swedish North Pole crossings in 1994 (e.g. TUCKER et al. 1999) and 2005 (e.g. PEROVICH et al. 2009).

Two of the most important sea-ice properties are its thickness and its degree of deformation, as they result from the integrative effects of the various growth and ablation processes and of external and internal forces which the ice experiences during its lifetime. They are indicators of changes of the ocean–ice–atmosphere and climate systems in the Arctic. Their local and regional distributions in turn affect growth, melt, and drift of the ice. In 1991, there were only two means of obtaining accurate ice thickness information: submarine upward-looking sonar (ULS) and drill-hole measurements. Although military submarine ULS provided accurate information over large regions, scientists had little influence on times and regions of data acquisitions, and often data were released only many years later and with blurred geographic information. Extensive drilling was therefore performed during ARCTIC 91 (see Fig. 7). However, although this was a key activity during this dedicated cruise, only 653 measurements could be obtained during 56 ice stations on as many floes (EICKEN et al. 1995).

As it became evident that ice thicknesses would change significantly with impending climate change, and because future "Polarstern" cruises would provide ideal conditions for systematic ice-thickness surveys, AWI-scientists subsequently looked for easier ways of ice-thickness measurement to obtain more

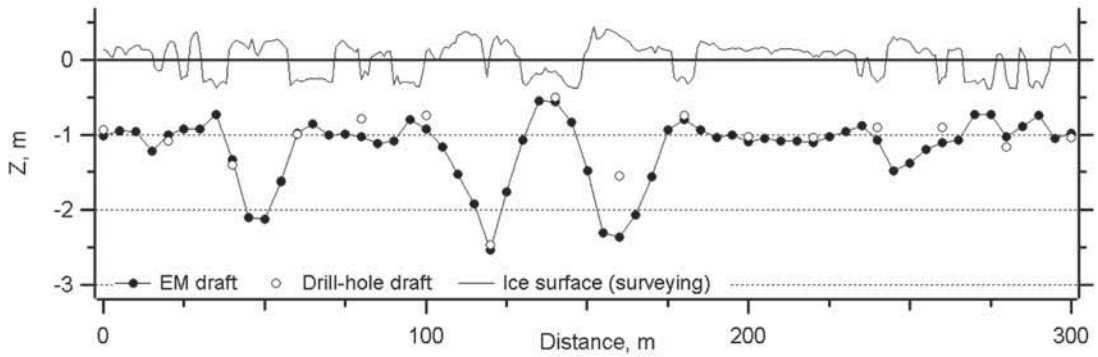

Fig. 10: Typical ice thickness profile of first-year sea ice measured during summer 1995 in the Laptev Sea, showing surface elevation and draft obtained by a combination of surface surveying, melt-pond depth sounding using a ruler stick, EM sounding, and drill-holes for validation (from HAAS & EICKEN 2001). The water level is at Z = 0 m. Negative surface elevation indicates location and depth of melt ponds.

Abb. 10: Typische Variationen der Eisdicke in einem Meereisprofil über einjährigem Meereis, gemessen in der Laptewsee im Sommer 1995. Die Abbildung zeigt das Oberflächenprofil und den Verlauf der Eisunterseite. Die jeweiligen Profile wurden durch die Kombination von Vermessungen der Oberfläche, Messungen der Tiefe von Schmelzwassertümpeln mit einem Messstab, elektromagnetischer Sondierung und Bohrungen zu Überprüfungszwecken gewonnen (aus HAAS & EICKEN 2001). Der Wasserspiegel liegt auf Z = 0 m; negative Werte des Oberflächenprofils zeigen die Positionen und Tiefen von Schmelzwassertümpeln an.

Fig. 11: Ice thickness measurements during ARK XVII/1, using a ground-based EM instrument housed in a kayak (Photo: J. Bareiss).

Abb. 11: Eisdickenmessungen auf der Expedition ARK XVII/1 mit einer in einem Kajak untergebrachten elektromagnetischen Sonde (Foto: J. Bareiss).

extensive surveys than could be obtained by drilling. Therefore, on four "Polarstern" expeditions in the years from 1993 to 1996, extensive studies of the suitability and performance of the geophysical methods of electromagnetic induction (EM) sounding and seismics using flexural waves were carried out. Although seismic measurements held some promise not only to retrieve ice thickness but also ice mechanical properties (HAAS 1997), EM sounding proved to provide most accurate and rapid measurements of level ice thickness in summer and winter, and good relative thickness estimates over deformed ice (HAAS et al. 1997, HAAS & EICKEN 2001). Through the active transmission of an electromagnetic field and induction of eddy currents in the conductive seawater under the resistive ice, this method senses the average electrical conductivity of the underground, which decreases with increasing ice thickness. Because the resistivity of snow and ice are both very high, these two media cannot be distinguished by EM measurements and the measured thickness corresponds to the total, ice plus snow thickness. Those "Polarstern" summer and winter expeditions provided ideal conditions for the validation and operationalizing of the EM method, and extensive comparisons with drill-hole measurements were performed (Fig. 10).

Because the EM method does not require contact with the ground and can be performed while moving, survey progress was improved by deploying EM instruments inside kayaks (Fig. 11), which served as amphibious sledges and allowed surveys across melt ponds. In 2001, average profile lengths of more than 2 km could be achieved during 54 ice stations. The method was subsequently also used from the ship while ice breaking, when an EM instrument was operated in front of "Polarstern" suspended 4 m above the ice with the bow crane (HAAS 1998).

Ice thickness from airborne electromagnetic sounding

Until 2001 ice-thickness measurements were limited to individual ice floes and could only be performed when the ice was thick enough to walk on. Therefore, in 1999 AWI scientists decided to develop an airborne EM sensor, which could be operated by helicopter (Fig. 12), and potentially with one of AWI's fixed-wing aircrafts. The sensor, named EM-Bird, was designed together with Aerodata AG (Braunschweig) and Ferra Dynamics Inc. (Canada). Besides the EM sounding devices for measuring the distance to the underside of the ice, the bird includes a laser altimeter to determine the distance to the ice surface (if the ice is covered by snow, it is the snow surface). The difference of those two measures is the ice (plus snow) thickness. The bird has to be towed 20 to 80 m under the aircraft to facilitate operation close to the ice where the measured EM fields are the strongest, and to avoid noise through induction in the metal of the aircraft. The first AWI EM-Bird was inaugurated during the "Polarstern" Arctic Mid-Ocean Ridge Expedition (AMORE) in 2001. Since then it

Fig. 12: Left: First flights with the EM-bird in the central Arctic Ocean in 2001. The bird is flown by helicopter 15 m above the ice surface (Photo: J. Lieser). Right: Since 2009, airborne EM ice thickness surveys are conducted with AWI's "Polar 5" airplane (Foto: C. Haas).

Abb. 12: Links: Erste Flüge mit der elektromagnetischen Sonde 2001 im zentralen Nordpolarmeer. Während des Hubschrauber-Fluges befindet sich die Sonde in einer Höhe von 15 m über dem Eis.
Rechts: Seit 2009 werden Flüge zur Eisdickenmessung mit elektromagnetischen Sonden auch mit AWI-Flugzeugen (hier "Polar 5") durchgeführt (Foto: C. Haas).

was used extensively not only during all "Polarstern" cruises into the Central Arctic Ocean and during the Ice Station "Polarstern" (ISPOL) and Winter Weddell Outflow Study (WWOS) projects in 2004 and 2006, respectively, but also from land-bases like Longyearbyen (Svalbard), Canadian Forces Station Alert (Canada), Barrow (USA), and even at the Russian North Pole Station Barneo. While surveys from land bases are limited by the range of the helicopters, "Polarstern" provides a mobile operating base and thus supports surveys over much larger regions than possible from land. In 2007, for example, more than 3000 km of profile data were collected.

A combination of electromagnetic sounding and laser altimetry for measurements of sea-ice thickness was also devised by PRINSENBERG et al. (2002). However, they tested the option of hard mounting the sensor on a helicopter instead of using a towed bird. Measurements by the fixed system are either carried out in "spot" mode (the helicopter remains over the same position during measurements, with its skids touching the ground) or in profiling mode (the helicopter is flown at very low altitudes). This way the level of necessary logistics is reduced, and the sensor's footprint on the ice is small. One major disadvantage is that such a system cannot be used on fixed-wing aircrafts.

Since 2009, the EM-Bird has been operated with AWI's "Polar 5" aircraft (Fig. 12), which now allows thickness surveys of more than 1000 km length during individual flights, and which can map most key regions of the Arctic within a few weeks (HAAS et al. 2010). However, the region of the North Pole and Eastern Arctic is still largely inaccessible by the range-limit of the aircraft, and future surveys will continue to rely on repeat visits by "Polarstern". Ship cruises also still offer unique opportunities for careful in-situ validation of the EM measurements by means of drill-hole and underwater ULS data, which require significant extra efforts during aircraft missions and can only be performed with ski-equipped planes.

During all thickness surveys in the 20 years since ARCTIC-91, AWI scientists and national and international collaborators have documented substantial changes, which are important for the understanding of the overall retreat of the sea-ice cover (Fig. 3). These are summarized in Figure 13. Modal (mean) ice thicknesses have decreased from 2.5 (3.11) m in 1991 to 0.9 (1.3) m in 2007 and 2011 (EICKEN et al. 1995, HAAS 2004, HAAS et al. 2008, Hendricks pers. comm.), i.e. by 64 % (mode) and 58 % (mean). The strongest drop occurred between 2004 and 2007. Because of the thinner ice "Polarstern" is now able to operate alone in the waters of the North Pole. Another effect was that the dramatic thinning substantially reduced the efforts required to perform validation and calibration drill-hole measurements. While in 1991 three auger sections of 1 m length had to be connected to drill through the ice, in 2001 the ice could be penetrated mostly with only two auger sections, and in 2007 one section was often enough!

In parallel to the efforts of the AWI-team to improve ice thickness observations in the central Arctic Ocean in the past 20 years, significant advances have been made by other groups with airborne laser altimetry (e.g. HVIDEGAARD & FORSBERG 2002, KWOK et al. 2012) and satellite laser and radar altimetry (e.g. KWOK et al., 2009, LAXON et al. 2003). These methods

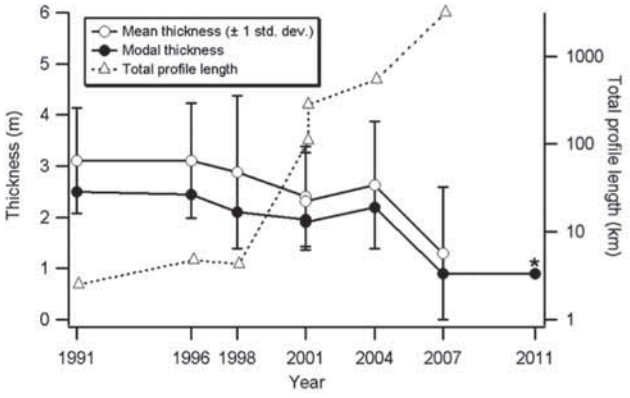

Fig. 13: Ice thickness change observed on "Polarstern" cruises to the central Arctic Ocean during the past 20 years. The increase in total profile length is also shown (dashed curve), and is due to improvements of the observational methods (1991 = drilling, 1996-2001 = ground-based EM-sounding, since 2001 = airborne EM sounding). Data from 2011 marked by an asterisk are courtesy of S. Hendricks (AWI).

Abb. 13: Änderungen der Eisdicke, beobachtet auf "Polarstern"-Expeditionen im zentralen Arktischen Ozean während der letzten 20 Jahre. Die Zunahme der gemessenen Profillängen ist ebenfalls gezeigt (gestrichelte Kurve). Sie ist Folge der technologischen Verbesserungen des Messverfahrens (1991 = einzelne Bohrungen, 1996-2001 = bodengebundene elektromagnetische Sondierung, 2001 und folgend = Sondierungen vom Hubschrauber oder Flugzeug). Die Daten von 2011, gekennzeichnet durch Sternchen, stammen von S. Hendricks (AWI).

obtain estimates of the snow or ice freeboard (i.e. the height of the snow or ice surface above the local water level), from which ice thickness can be calculated based on assumptions of isostatic equilibrium, the thickness of the snow, and the densities of snow and ice. Between 2004 and 2008, the laser altimeter measurements of NASA's ICESat satellite showed similar amounts of thinning as found during the "Polarstern" expeditions, but provided more extensive information because it covered the complete Arctic Ocean twice per year (KWOK et al. 2009). Using the radar altimeter aboard ESA's Envisat, GILES et al. (2009) showed the regional extent of the strong thinning between the winters of 2004–2007 and 2008, which corresponded to the strong thinning observed by the "Polarstern" in the summer of the same time period (HAAS et al. 2008). In 2010, ESA launched the CryoSat satellite, dedicated to observe thickness changes of Arctic and Antarctic sea ice with an improved, synthetic-aperture radar altimeter (WINGHAM et al. 2006).

The strong sea-ice thinning is not only caused by thermodynamic changes, but also by changes in ice drift and dynamics which have led to reductions in the amount of old, thick ice in the Arctic Ocean (e.g. KWOK et al. 2009, MASLANIK et al. 2011). Satellite passive-microwave and scatterometer observations have been instrumental in these observations, which are facilitated by the differences between microwave properties of first- and multi-year ice. In particular, these data show that

- in 2007 the region of the North Pole was covered only by first-year ice for the first time since satellite observations were available in 1979,
- thick multi-year ice has retreated into a narrow band off the coasts of Greenland and Canada, and
- the majority of the Arctic Ocean is now covered by first- and second-year ice only.

This means that today research vessels such as "Polarstern"

can traverse and investigate most regions of the Arctic Ocean with relative ease, and that multi-ship expeditions are no more required for operational reasons alone.

THE USE OF IMAGING RADAR FOR SEA-ICE MONITORING

Sea ice observations with the ERS-1 radar systems

In conjunction with the launch of ERS-1, a number of projects were started that focused intensively on research topics related to radar remote sensing of sea ice. Topics included:

- experimental and theoretical investigations of radar wave scattering from sea ice,
- ground-based and airborne field campaigns for collecting radar signatures typical for different ice types and ice conditions,
- development of image processing algorithms specifically adapted to sea ice observations, and
- the implementation of operational sea ice monitoring strategies.

The ERS-1 satellite carried different radar systems and other instruments on board. The synthetic aperture radar (SAR) was used to collect images along a 100 km wide swath with a horizontal resolution of 30 m. Such a high resolution requires a large antenna that cannot be mounted on a satellite. The notation "synthetic aperture" indicates that a long antenna is "synthesized" when processing the raw data that are measured by the shorter physical antenna. The so-called (radar) scatterometer measures the intensity reflected from the Earth's surface at a much coarser resolution of 48 km. This instrument type has been applied, for example, to derive large-scale ice drift-patterns over the entire Arctic and Antarctic. The third radar instrument on ERS-1 was an altimeter. Its data were applied for retrieving ice thickness (as mentioned above) and for the mapping of sea-ice extent.

Comparing and combing data from different satellite radar systems

In 1995, two more satellites with imaging radars on board were launched: the European ERS-2 (with the same radar instruments as ERS-1), and the Canadian RADARSAT. The latter used radar signals at a polarization different from ERS-1/2. With the SAR system of RADARSAT it became possible to select a number of imaging ("beam") modes that differed in swath width (50-500 km), spatial resolution (8-100 m), and the viewing angle relative to nadir (selectable in the interval 10-59°). This flexibility made it possible to acquire image series with higher temporal resolution than with ERS-1/2. ERS-1 was taken out of operation in 2000, ERS-2 in 2011. In 2002, ESA launched ENVISAT, which – besides other instruments – carried an advanced SAR (ASAR) and a radar altimeter on board, but no scatterometer. Communication with ENVISAT was lost in 2012. Also the ENVISAT ASAR provided options to select different imaging geometry, and in addition different polarizations of the radar signal. All those SAR systems were using the same radar frequency (C-band, wavelength 5.7 cm). The SAR on SEASAT, which was the first satellite designed for monitoring ocean regions, was operated at L-band (wavelength 25 cm). Unfortunately, the mission ended abruptly in 1978 after only four months duration because of a short circuit in the satellite's electrical system. Also the Japanese satellites JERS-1 (1992-1998) and ALOS (2006-2011) were equipped with an L-band SAR. Shorter wavelengths (X-band, wavelength 3.1 cm) are used for the German TerraSAR-X (in space since 2007). Typical for the recent satellite missions is the much larger flexibility in selecting different modes for image acquisitions.

This (incomplete) list of satellites carrying imaging radars is an example for the development of space technology, which has considerably improved the information retrieval of state and variations of the polar sea-ice covers. Sea ice remote sensing does not only benefit from more and more advanced radar sensors but also from progress in the technology of other space-borne, airborne, and ground-based instruments – as the example of sea-ice thickness measurements pictured above demonstrates.

The combination of satellite, airborne, and ground-based data acquisitions

Comparisons of satellite SAR imagery with optical and radar images acquired at a high spatial resolution from airplanes are extremely useful to assess the potential of different radar configurations for ice-type classification. In the high-resolution low-noise images of aircraft instruments, many structural details of the ice cover can be identified. An example of airborne multi-polarization images acquired by an airborne SAR system at C- and L-band is shown in Figure 14. Aerial photography provides the means for the interpretation of the radar data. A problem, however, is that sea ice is often covered by snow which means that no information can be obtained about the ice structure beneath the snow from photos taken in the visible or infrared. This is a great advantage of radar: if the snow is dry, radar can look through it. The strategy of combining optical and radar aircraft and satellite images was used, for example, in a field campaign around Svalbard. The objective was to assess the technical performance of the European Space Agency's Sentinel-1 SAR mission for sea-ice mapping (DIERKING 2010).

For a direct comparison of different radar configurations, ground-based measurements offer the advantage that sea-ice properties affecting the radar waves can be directly measured concurrently – one only has to make sure that the work on the ice does not interfere with the radar measurements from the ship. A comparison of radar systems that operate at different wavelengths was, e.g., carried out by DIERKING et al. (1999) in the Baltic Sea. Their measurement results indicated that a number of different interaction mechanisms between sea ice and radar waves were effective. Both surface and volume scattering mechanisms have to be taken into account, but their relative contributions depend on the radar frequency. DIERKING et al. (1999) found, for example, that the radar intensities at X-band (3 cm wavelength) were mainly influenced by the air bubbles in the subsurface ice layer, at C-band (5.7 cm) by the centimetre-scale surface roughness, and at L-band (25 cm) by the structure of the ice-water interface. The latter result is special for the Baltic Sea where ice does not survive the summer melt (i.e. it is first-year ice) and its salinity is between 0 and 2 psu (practical salinity units). In the Arctic and the Antarctic, the salinity of

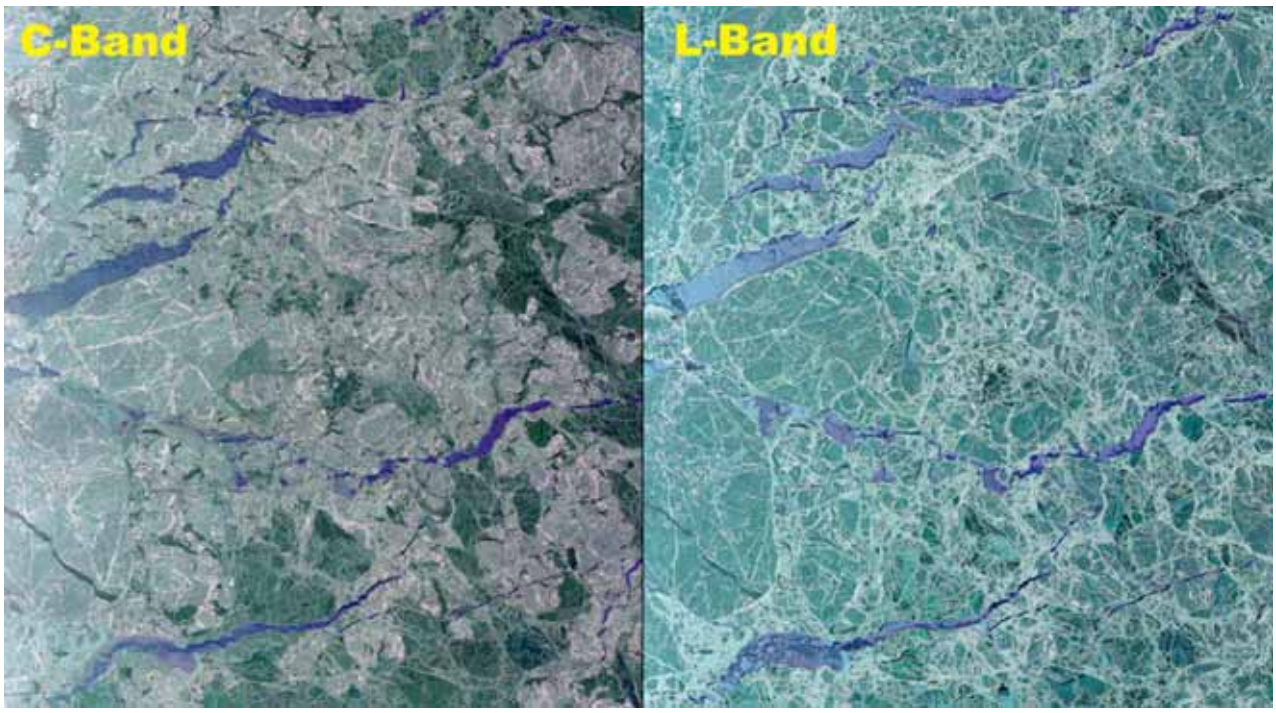

Fig. 14: Airborne radar images of sea ice north of Svalbard, acquired at a frequency of 1.25 GHz (L-band) and at 5.3 GHz (C-Band). The image width corresponds to 12 km. At each frequency data were measured at different polarization combinations (HH, HV+VH, VV, V = vertical, H = horizontal, first letter = transmitted signal, second letter = received signal). The colour images are composed of three layers (red, green, blue: RGB, with R-HV+VH, G-HH, B-VV). Bluish areas are thin ice and open water. Dark green patches at C-band (upper image) indicate young ice, light green patches older ice. Bright lines and patterns in the radar images are ridges and deformation zones, respectively (Courtesy: Technical University of Denmark).

Abb. 14: Luftbilder, aufgenommen mit verschiedenen Radarsystemen über dem Meereis nördlich von Spitzbergen. Die Radarsysteme wurden mit Frequenzen von 1.25 GHz (L-Band) und 5.3 GHz (C-Band) betrieben. Die Breite der Bilder entspricht einer Strecke von 12 km. Die Daten wurden in verschiedenen Polarisationskombinationen aufgenommen (HH, HV und VH, VV; V = senkrecht, H = waagerecht; erster Buchstabe = abgestrahltes Signal, zweiter Buchstabe = empfangenes Signal). Die Farbbilder sind aus drei Ebenen (RGB, rot-grün-blau) zusammengesetzt, denen die Polarisationskombinationen wie folgt zugeordnet wurden: R-HV+VH, G-HH, B-VV. Blaue Flächen sind dünnes Eis und offenes Wasser. Die dunkelgrünen Flächen im C-Band (oben) stehen für junges Eis, hellgrün bedeutet älteres Eis. Die hellen Linien und Muster sind Eisrücken und zerbrochene und/oder zusammengeschobene Eisflächen (Quelle: Technische Universität Dänemark in Lyngby).

first-year ice varies from 5 to 12 psu, and the influence of the ice-water interface on the measured radar signal, which depends on ice salinity and thickness, is much weaker. At this point one could ask whether the knowl-edge about scattering mechanisms and their relative contributions is necessary in such detail? The answer is definitely yes. This knowledge is the basis for any interpretation of radar signatures observed in satellite images, and, going one step further, it is needed to develop methods for sea-ice type classification and for the extraction of information on geophysical parameters related to the ice conditions, for example the onset of melt (see below).

The disadvantage of ground-based radar measurements is that they are restricted to a few small spots on the ice. With air- and space-borne image acquisitions larger areas with different ice conditions and ice types can be covered within short time intervals. But considering the logistic problems in ice-covered waters, it is often difficult to get the field crew into the view of the satellite or aircraft at a scheduled time. Airborne measurements are more flexible with respect to the flight path, but it depends much on the weather conditions whether they can be carried out. Satellites fly on orbits fixed in space and time.

One important aspect of combining ground, airborne and satellite measurements is the possibility of upscaling or downscaling. Related issues are, for example: how does the coarser spatial resolution of a satellite sensor affect the capability to separate different ice types? In which way is the local ice state observed on the ground or from the airplane influenced by regional conditions, which can only be determined from satellite images because of their wider imaging swath? Is it possible to devise algorithms by which geophysical parameters can be retrieved on sub-pixel scale?

Ice type separation in radar images

One central question that arose in particular for operational ice mapping services was how well one can separate different ice types in SAR images. For getting an answer, STEFFEN & HEINRICH (1994) used ERS-1 and optical images of the Landsat Thematic Mapper from the Beaufort Sea. First- and multi-year ice revealed different radar intensity ranges and could be clearly distinguished. If frost flowers (Fig. 15) covered the surface of young ice, the radar intensity was much higher compared to a bare ice surface. Ice-free areas in the pack ice could be reliably detected only under calm wind conditions or at wind speeds >10 m s^{-1}. This can be explained as follows: The wind generates small ripple waves (lengths millimetres to decimetres) on the water surface. The backscattered radar

intensity is the larger the rougher a surface is. Hence, the radar intensity of an open water surface may be very similar to the ice at certain wind speeds. The highly variable radar signatures of open water are in fact one of the challenges in automatic mapping of sea-ice conditions.

FETTERER et al. (1994) investigated the quality of ice type maps from the Arctic that were automatically generated using radar intensity as classifier. They found that first-year ice and multi-year ice could be separated with high accuracy, but the algorithm sometimes failed to correctly classify open water and new ice as well as smooth and rough first-year ice. It is important to note that the radar intensities measured for different ice types and their relative differences are a function of radar frequency, polarization, and incidence angle. In the case of ERS-1, none of those parameters could be varied. Another important point is that the radar intensity of sea ice changes partly drastically with the onset of melt (see below). In the investigations by STEFFEN & HEINRICH (1994) and FETTERER et al. (1994), the images used for the analyses were acquired under freezing conditions.

Ship-based radar measurements combined with ground-based laser-profiling of the ice surface revealed a strong sensitivity of the observed radar intensity to the surface roughness at centimetre- to decimetre-scale (DIERKING et al. 1997), such as shown in Figure 9. Frost flowers (Fig. 15), saline snow, and slush on the ice surface can considerably influence the backscattered radar intensities. This effect was investigated in more detail by ULANDER et al. (1995), who used ERS-1 images and developed a theoretical scattering model on the basis of in-situ data from the ARCTIC 91 expedition. They found that surface scattering dominated the radar signal and that different surface

Fig. 15: Sampling of frost flowers on sea ice (Photo: W. Dierking).

Abb. 15: Beprobung von Raureif auf dem Meereis aus einem Personenkorb vom Schiff aus (Foto: W. Dierking).

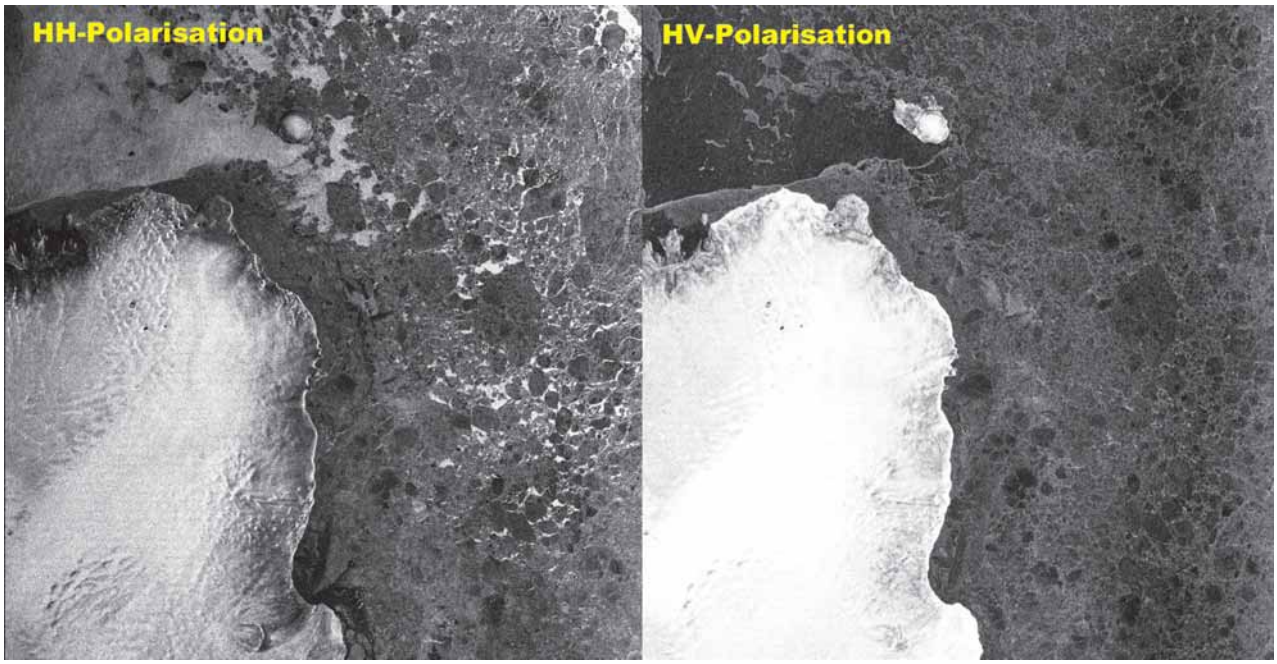

Fig. 16: Envisat ASAR images over sea ice (appearing greyish) and land ice (bright) around the northeast tip of Nordaustlandet (Svalbard), acquired at two different polarizations. The images cover an area of 100 km x 100 km. The area in the upper left corner is to large part open water. It appears bright at HH-polarization and dark at HV-polarization. "H" and "V" denote horizontal and vertical polarization of the radar signal, respectively; "HV", for example, means that the transmitted signal is horizontally and the received signal vertically polarized (Copyright: ESA).

Abb. 16: Envisat ASAR-Bilder, aufgenommen über der nordöstlichen Spitze von Nordaustlandet (Spitzbergen). Das Bild zeigt Meereis (Grautöne) und Landeis (hell bis weiß). Die Bilder wurden in zwei verschiedenen Polarisationskombinationen aufgenommen und entsprechen einer Fläche von 100 km x 100 km. Das Gebiet links oben ist zum größten Teil offenes Wasser, das im HH-polarisiertem Bild hell und im HV-polarisierten Bild dunkel erscheint. (H = waagerechte, V = senkrechte Polarisation, "HV" bedeutet z. B., dass das abgestrahlte Signal waagerecht und das empfangene Signal senkrecht polarisiert ist), (Copyright: ESA).

conditions caused large variations in the appearance of young ice in the ERS C-band images. At L-band, for example, the influence of frost flowers on the radar signal is much weaker (DIERKING 2010).

Figures 14 and 16 show examples of radar images taken over sea ice that differ in frequency and polarization. If they are combined, more ice classes can be distinguished than with single-frequency single-polarization radar. It is also easier to separate open water and ice (Fig. 16). Hence it is in principle beneficial for operational sea-ice mapping to combine the imagery of different satellite radars. But economical questions concerning the costs for data acquisitions, processing, and map production have also to be addressed in this context. Therefore basic research is needed to assess the pros and cons of various combinations of radar imaging configurations. When using two or more satellites to observe a given area on the Earth's surface, the time of over-flight varies from satellite to satellite. Since ice drift-speed may be considerable (dependent on wind and ice conditions; at the ice margin, for example, 30 km d^{-1} are not unrealistic), a temporal difference of a few hours may be too long for a meaningful image combination (in particular for narrow swath width <100 km).

DIERKING & BUSCHE (2006) compared images from two satellites. They focused on data from SAR systems on ERS-1 (C-band) and JERS-1 (L-band) that were acquired at the east coast of Greenland and south of Svalbard with time differences of 25 and 35 minutes, respectively. They had to consider that the instruments did not only differ in frequency but also in their polarization and look angle. Another problem was the lack of any in-situ sea-ice data. Nevertheless, they could demonstrate that the information content of both radar systems is complementary. Zones of ice deformation and smooth level ice floes are much easier to separate at L-band, but first- and multi-year ice can be better distinguished at C-band.

Which ice surface properties can be obtained from SAR images?

The ice surface structure is characterized by, for example, distances between ridges, ridge heights, floe sizes, ice concentration, and ice freeboard. Knowledge about these parameters is valuable for studies of the wind drag and wind turbulence in the atmospheric boundary layer which can be as shallow as 50 m over sea ice (DIERKING 1995, GARBRECHT et al. 1999, GARBRECHT et al. 2002). Building on the experience with laser profiling of the sea-ice surface topography gathered during ARCTIC'91, AWI-scientists focused on the question whether satellite SAR data could be used to derive the mean ridge spacing in a given area. To this end, the intensity variations in ERS-1 images were compared to laser profiles measured from a helicopter (HAAS et al. 1999). It was found that the mean radar intensity was higher when more ridges per unit area were present. However, the correlations between intensity and ridge frequency were unfortunately only poor.

It is not possible to retrieve variations of surface height directly from SAR images. This does not mean that it is not worthwhile to take SAR images as data source for questions related to ice surface structure. One example is to complement height measurements ("vertical structure") from laser profilers (one-dimensional) or laser scanners (two dimensional along a narrow strip) with information about horizontal ice deformation patterns (two-dimensional along a wider strip) from satellite images. If the spatial resolution of a SAR image is sufficiently high, it is possible to identify single ice floes and

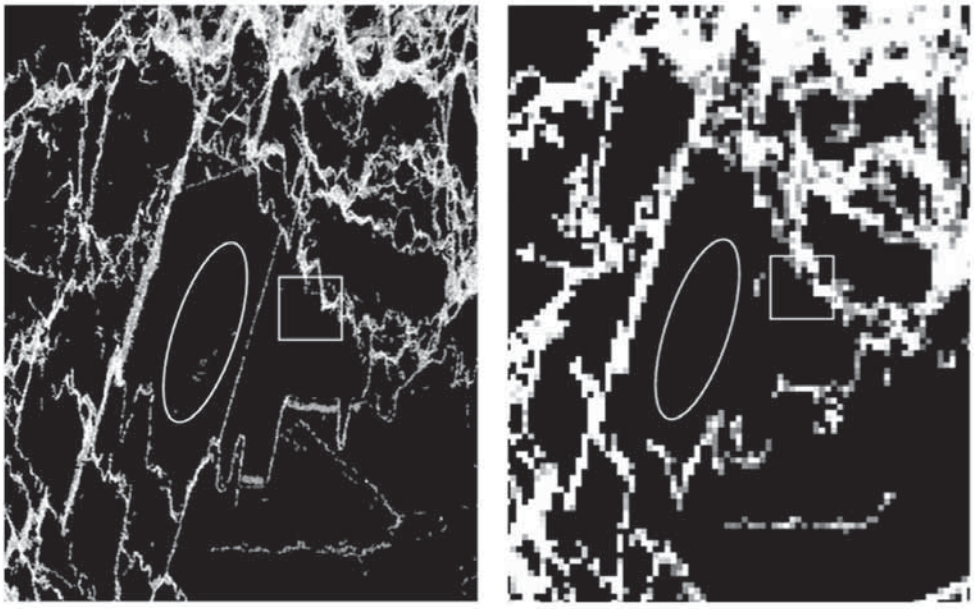

Fig. 17: Ice ridges detected in an airborne L-band SAR image (left = pixel size 5 m, right = 25 m). Demonstrated is the target loss (ellipse) and the image smear (rectangle) at coarser spatial resolution. From DIERKING & DALL (2008).

Abb. 17: Detektierte Eisrücken in einem vom Flugzeug aus aufgenommenen SAR-Bild (Pixelgröße links = 5 m, rechts = 25 m). Gezeigt ist der Verlust eines Objekts (in der Ellipse) und die "Verschmierung" von Bildelementen (Rechteck) in dem Bild mit schlechterer Flächenauflösung (rechts). Aus DIERKING & DALL (2008).

zones of deformation (Figs. 14, 16, 17). Whether the resolution is "sufficient" depends in general on which spatial scales the parameter of interest changes its value. The size of ice floes, for example, lies between about 10 m ("small floe") and more than 10 km across ("giant floe"). The width of ridges (as seen on the ice surface) can vary from less than a meter up to more than 20 meters. DIERKING & DALL (2007, 2008) found that ice ridges and rafting zones (which occur in thin ice) are preferably mapped using L-band SAR images at high spatial resolution of 5–10 m (Fig. 17). However, even at coarser resolution (25–30 m), the major deformation patterns can be clearly distinguished, although narrow ridges and rafting zones are lost in the image, whereas the remaining structures appear broader due to image "smear". The influence of radar polarization and incidence angle on detection is only minor.

Surface properties differ depending on ice conditions and ice types. Hence, the information on ice types, as discussed above, is useful for categorizing the ice surface structure. Also valuable in this context is ice freeboard that can be obtained if the ice thickness is known. One question of interest has been whether it is possible to relate ice thickness or freeboard to the measured radar intensity? Among remote sensing specialists it was clear from the beginning that a direct relationship does not exist. Radar signatures are predominantly influenced by millimetre-to-decimetre scale surface and volume properties of sea ice. So the question is whether such properties differ between different ice types. (One criterion for separating ice types is their thickness). BUSCHE et al. (2005) compared thickness measurements carried out with an EM-bird attached to a helicopter with the radar signatures along the flight path obtained from a satellite SAR image (Fig. 18). The problem was to compensate the effect of the ice drift that occurred between helicopter measurements and satellite over-flight, since no corresponding information was available. The direct correlation between radar intensity and ice thickness revealed only a low correlation. With modern SAR systems it is also possible to use the intensity ratio between differently polarized signal channels (specifically HH- and VV-polarization; see Fig. 14 for an explanation of the denotation). In one study, ice thickness could be retrieved from ENVISAT ASAR C-band data based on the polarization ratio VV/HH (NAKAMURA et al. 2009), but only for ice that was less than 1.2 m thick. In general, multi-polarization SAR systems operated at L-band are better suited for thickness retrievals (NAKAMURA et al. 2006) but the restriction to thinner ice applies also in this case. All in all, no robust, generally valid method exists to determine the ice thickness directly from SAR data.

THE MELTING SEASON

A large part of the ARCTIC 91 cruise was carried out under melting conditions as Figure 6 demonstrates. How do such conditions affect the microwave properties of sea ice? In fact, the change of microwave properties is significant. WINEBRENNER et al. (1994) observed a distinct decrease of the radar intensity scattered from multi-year ice at the onset of melt such as shown in Figure 19. Multi-year ice is character-ized by the presence of air bubbles in the upper ice layers. Radar waves that penetrate into the ice are scattered by those bubbles. However, radar signals of perceptible intensity propagate through the ice volume only if temperatures are below freezing and the ice surface is dry. When the ice surface starts to melt, the radar penetration depth is drastically reduced and the level of volume scattering from air bubbles is very low. This decrease of the received radar intensity is also visible in the images of SAR systems operated at other frequencies. The reverse process is observed during autumn. When temperatures fall below freezing, the volume scattering contribution increases strongly and rapidly (WINEBRENNER et al. 1996). KWOK et al. (2003) used images from the Canadian RADARSAT to study the timing of melt-onset over the entire Arctic sea-ice area. They found that the radar intensity from first-year ice increases with the onset of melt. For melt detection, they developed an algorithm that uses not only changes of radar intensity but also additional criterions related to the distribution of radar intensity values in an area of 5 × 5 km^2 (including 2500 pixels). The algorithm was validated by comparing the timing of melt onset obtained from RADARSAT data with the zero crossings of buoy temperature records. The corresponding dates differed by 1–2 days. KWOK et al. (2003) noted that the timing of melt onset derived from passive microwave data occurs later, i.e. it is biased to a

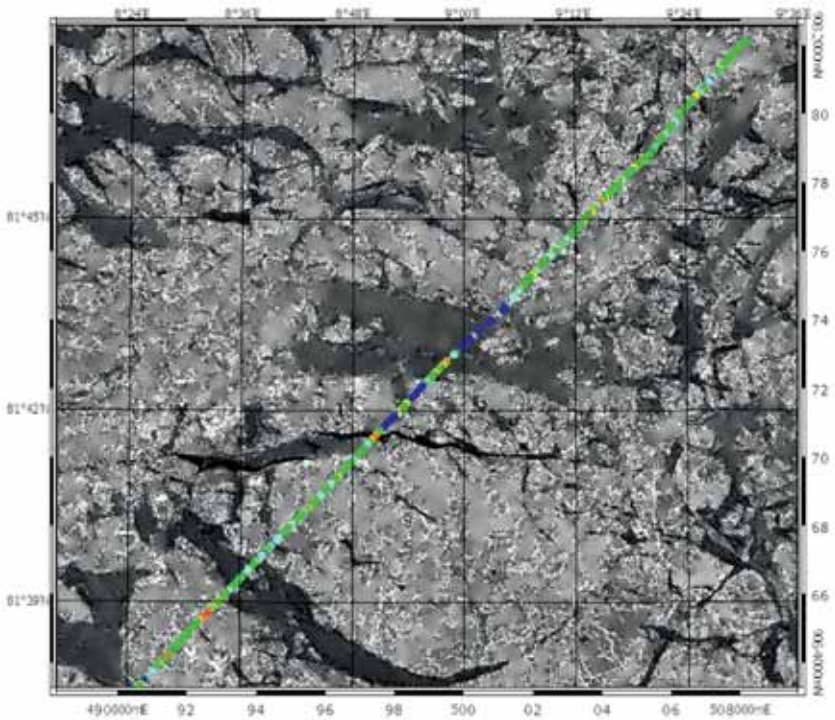

Fig. 18: Radarsat-1 SAR image showing a mix of first- and multiyear ice in Fram Strait, with ice thickness obtained by helicopterborne EM sounding overlayed (from BUSCHE et al. 2005).

Abb. 18: Radarsat-1 SAR Bild aufgenommen über ein- und mehrjährigem Eis in der Framstraße. Die mittels elektromagnetscher Sondierung vom Hubschrauber gemessene Eisdicke ist als farbiges Profil darüber gelegt (aus BUSCHE et al. 2005).

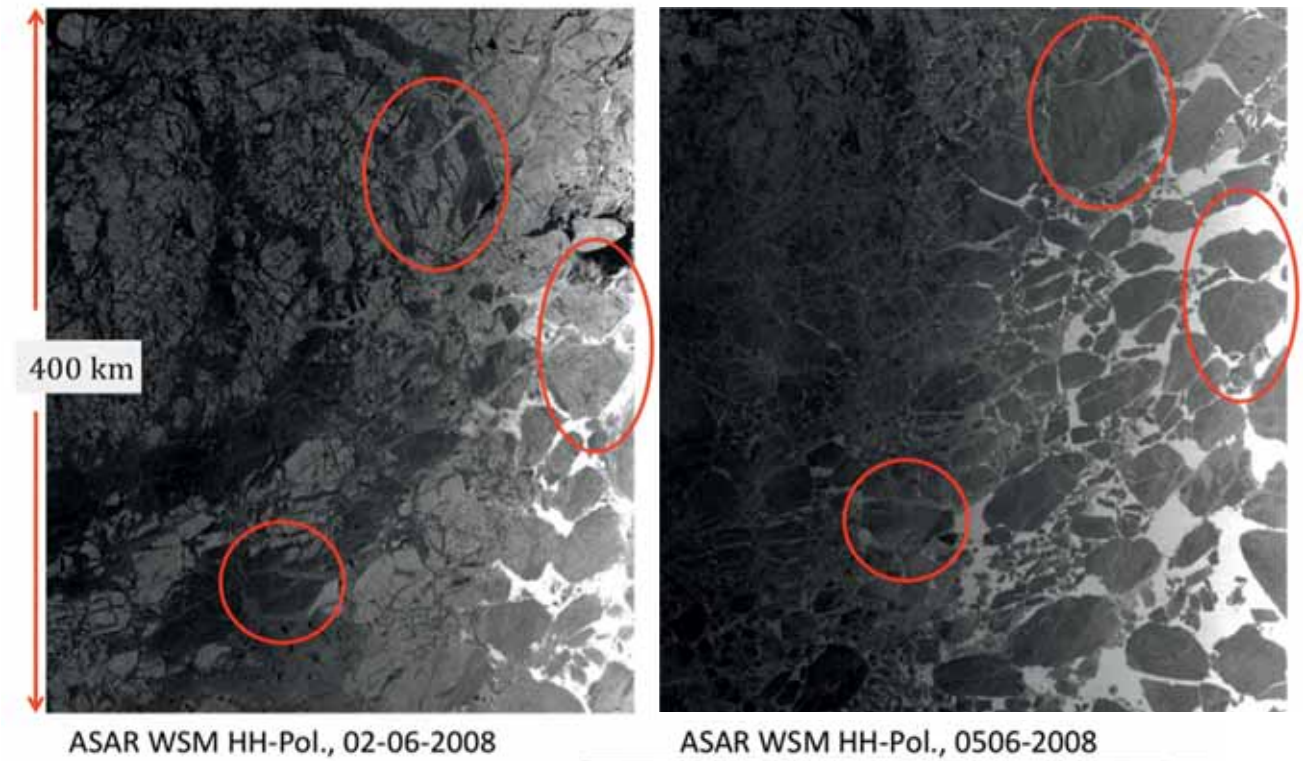

Fig. 19: Sea ice in the Beaufort Sea (71-76° N, 130–150° W). The left image was acquired in the beginning of June 2008, when air temperatures were below zero; the right image was acquired three days later after the onset of melting conditions. The red ellipses mark arbitrarily selected ice structures as references in both images for ease of comparison. Under melting conditions, the radar intensity backscattered from the ice changes, and the separation of young and old ice becomes more difficult. (Copyright: ESA).

Abb. 19: Meereis in der Beaufort-See im Frühjahr 2008. Das linke Bild stammt von Anfang Juni, als die Temperaturen unter Null Grad lagen. Das rechte Bild wurde drei Tage später aufgenommen, nachdem die Eisschmelze eingesetzt hatte. Die roten Ellipsen kennzeichnen willkürlich gewählte Eisstrukturen, um die Orientierung in beiden Bildern zu erleichtern. Unter Schmelzbedingungen ändert sich die empfangene Radarintensität, und die Unterscheidung von jungem und altem Eis wird schwieriger. (Copyright: ESA).

later stage of melt. This has to be considered when comparing dates of melt onset and freeze-up obtained from SAR and microwave radiometer data. The latter proved to be extremely useful for deriving an Arctic-wide view of melting patterns covering the last three decades. MARKUS et al (2009) used passive microwave data to determine the timing of melt onset and freeze-up and the length of the melt season from 1979 to 2007. For the entire Arctic, the melt season length increased on average by 20 days, but regional differences are relatively large (Fig. 20). The largest trends of more than ten days per decade were found in the East Greenland Sea, Laptev Sea, and East Siberian Sea, Chuckchi and Beaufort Sea, and Hudson Bay.

THE FUTURE

Sea ice is one of the "Essential Climate Variables" (ECVs) as defined by the Global Climate Observing System (GCOS) Steering Committee. In the report "The Changing Earth" (ESA 2006), the main research challenges listed for sea-ice research are

- to quantify the distribution of sea ice mass and freshwater equivalent;
- to assess the sensitivity of sea ice to climate change, and
- to understand thermodynamic and dynamic feedbacks between ocean, sea ice, and atmosphere.

The importance of improved sea-ice observations (in-situ, airborne, from space) is mentioned also in other documents, among them the "IPCC Report on Climate Change" (LEMKE et al. 2007), the "Arctic Climate Impact Assessment" report (ACIA 2004), and the" Cryosphere Theme Report of the Integrated Global Observing Strategy" (IGOS 2007).

Sea-ice observations need to include ice extent, the ice edge, ice concentration, ice type distribution, leads and polynyas, ice thickness, snow depth on sea ice, and ice drift. Since sea ice is subject to rapid temporal and spatial variations, monitoring from space is required, which enables a complete coverage of the Arctic (or Antarctic) and short repeat intervals at medium to low spatial resolution (100 m - 10 km). For future sea-ice observations, various space missions will be employed, among them:

- Sentinel-1 (SAR),
- MetOp-SG (scatterometer, radiometers operating in the visible, infrared and microwave range),
- Cryosat-2 and Sentinel-3 (radar altimeters), and
- ICESat-2 (laser altimeter).

The Sentinel missions have been developed by ESA specifi-

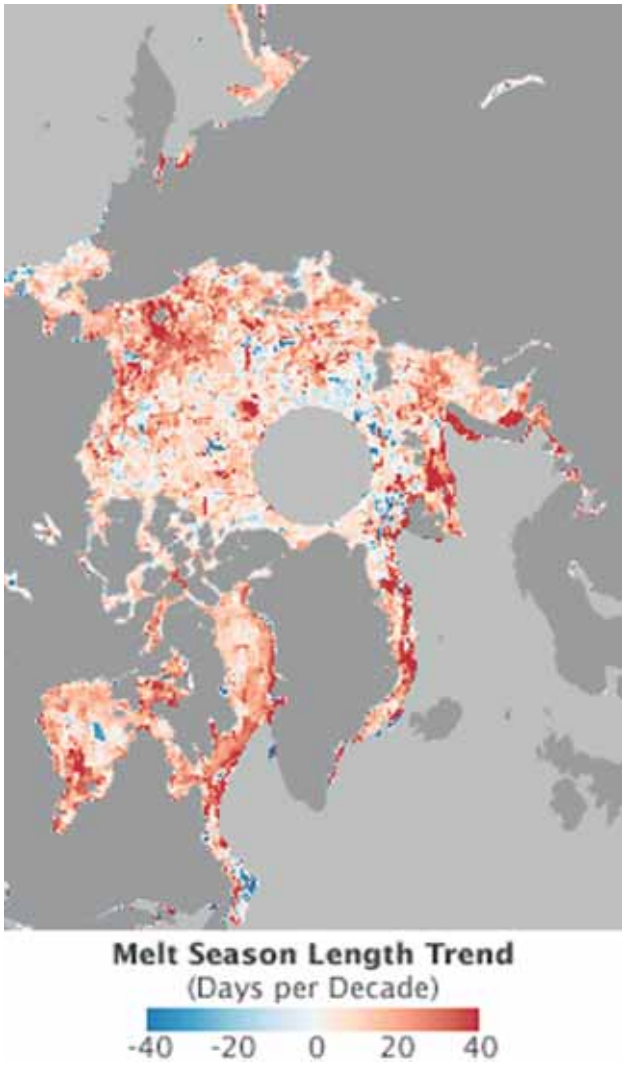

Fig. 20: Regional changes of melt season length over the Arctic from 1979 to 2007, derived from passive microwave data over sea ice (NASA Earth Observatory, http://earthobservatory.nasa.gov/IOTD/view.php?id=42456).

Abb. 20: Regionale Änderungen der Dauer der Schmelzsaison in der Arktis zwischen 1979 und 2007, abgeleitet aus über dem Meereis aufgenommenen Daten von passiven Mikrowellenradiometern (Quelle: NASA Earth Observatory).

cally for the needs of the GMES (Global Monitoring for Environment and Security) initiative. They are based on a constellation of two satellites to fulfill the GMES revisit and coverage requirements. There are five different Sentinels for monitoring of land, oceans, and atmosphere. The launches of the first satellites for Sentinels 1–3 are scheduled for 2013. The MetOp (Meteorological Operational satellite) series, consisting of satellites A to C (launches 2006, 2012, and 2016) and MetOp-SG (Second Generation, starting 2018) provide space observations of temperature, humidity, ocean surface wind speed, sea ice drift, and ozone and trace gases at global scale. The "Ice, Cloud and land Elevation Satellite-2" (ICESat-2) will be used for the estimation of sea ice thickness and ice sheet elevation changes, among other tasks. It will be launched in 2016. For local and regional studies, which require a higher spatial resolution, a number of missions already operational (such as RADARSAT-2) or under development will provide the necessary data.

Among those sea-ice parameters that need to be determined from satellite data, ice thickness is still most demanding with respect to the robustness and accuracy of the retrieval methods. Ice thickness will be monitored by means of radar and laser altimetry missions (see above). Radar altimeter measurements result in relatively large errors for ice that is thinner than 1 m (Laxon et al. 2003). Estimates of ice thickness from freeboard measurements using laser systems reveal errors of ±0.5 m (Kwok et al. 2009). Altimeters may be favourably complemented by passive microwave radiometers operated at L-band, such as ESA's SMOS (Soil Moisture and Ocean Salinity) mission. It was demonstrated with SMOS data that the change of emission during the different stages of sea-ice growth is large enough to retrieve ice thickness up to 0.5 m if air temperatures are below -10 °C (Kaleschke et al. 2012). The accuracy of thickness retrievals from satellite instruments depends on the knowledge of snow thickness and snow and ice density, as mentioned above. Their actual values at the timing of data acquisition are usually not known. Another problem is that the spatial resolution of the satellite radar altimeters (Cryosat-2: about 250 m along-track but up to 1 km across-track in the so-called SAR mode) is moderate, and for radiometers (SMOS: 35–45 km) it is coarse. This means that insights into the mechanisms of ice thickness variations cannot easily be gained because pressure ridges and narrow leads can hardly be separated from level ice.

This example shows that high-resolution airborne data acquisitions or in-situ measurements during ship expeditions remain mandatory also in the future for providing detailed data on sea-ice properties and processes. Other examples are the various physical and biogeochemical interaction mechanisms between the sea-ice cover and the atmospheric boundary layer, and between sea ice and the underlying water column. The authors expect that the availability of modern icebreaker technology and the better accessibility of the Arctic Ocean due to its thinner ice cover will make it possible to extend the time window for field campaigns from early spring to late autumn. This would mean that the sea-ice data measured in-situ, which hitherto are mainly from summer seasons, can be extensively supplemented by ice properties data that also reflect colder conditions.

SUMMARY

This brief and incomplete historic journey through sea-ice research and sea-ice remote sensing during the past twenty years touched topics that have been keeping the authors (and many others) busy since 1991. Those topics included in particular the ground-based and airborne measurements of sea-ice thickness and the use of satellite data for mapping sea-ice conditions, for characterizing the ice surface structure, and for determining melt-onset and freeze-up in the Arctic. Many other important issues could not be mentioned here. But the authors hope that they could provide at least a basic idea on how measurement technologies developed, and how the knowledge about sea-ice properties and interaction mechanisms between atmosphere, sea ice, and ocean has been extended during the past twenty years.

ACKNOWLEDGMENT

We thank D.K. Fütterer for the invitation to write this article on the occasion of the 20th anniversary of the ARCTIC 91 expedition, which was celebrated with a scientific symposium in Kiel and a get-together on a ferry between Kiel and Gothenburg in September 2011. The authors remember the fruitful collaborations with many colleagues during the ARCTIC 91 expedition, among them Hajo Eicken, Peter Lemke, Rolf Gradinger, Dirk Nürnberg, Stefan Härtling, Ursula Wieschollek on "Polarstern", and Anders Carlström, Lars Ulander, and Thomas Thompson on "Oden". Long-lasting collaborations and friendships still exist with many of these colleagues. Finally we would like to thank Dirk Nürnberg and an anonymous reviewer for their comments, which helped to improve the manuscript.

References

ACIA (2004): Impacts of a warming Arctic: Arctic Climate Impact Assessment. - Cambridge University Press, 1-140.

Bourke, R.H. & Garrett R.P. (1987): Sea ice thickness distribution in the Arctic Ocean.- Cold Reg. Sci. Technol. 13(3): 259-280.

Busche, T., Saldern, C., Haas, C. & Dierking, W. (2005): Comparison of helicopter-borne measurements of sea ice thickness and surface roughness with SAR signatures.- Proc. 2004 Envisat & ERS Symposium, European Space Agency, ESA SP572.

Carlström, A. & Ulander, L.M.H. (1993): C-band backscatter signatures of old sea ice in the central Arctic during freeze-up.- IEEE Transact. Geosci. Remote Sensing 31: 819-829.

Comiso, J.C. (2012): Large decadal decline of the Arctic multiyear ice cover.- J. Climate 25: 1176-1193, doi: 10.1175/JCLI-D-11-00113.1.

Dierking, W. (1995): Laser profiling of the ice surface topography during the Winter Weddell Gyre Study 1992.- J. Geophys. Res. 100(C3): 4807-4820.

Dierking, W. (2010): Mapping of different sea ice regimes using images from Sentinel-1 and ALOS synthetic aperture radar.- IEEE Transact. Geosci. Remote Sensing 48(3): 1045-1058, doi:10.1109/TGRS.2009.2031806.

Dierking, W. & Busche, T. (2006): Sea ice monitoring by L-Band SAR: an assessment based on literature and comparisons of JERS-1 and ERS-1 imagery.- IEEE Transact. Geosci. Remote Sensing 44(2): 957-970, doi:10.1109/TGRS.2005.861745.

Dierking, W., Carlström, A. & Ulander, L. (1997): The effect of inhomogeneous roughness on radar backscattering from slightly deformed sea ice.- IEEE Transact. Geosci. Remote. Sensing 35(1): 147-159.

Dierking, W. & Dall, J. (2007): Sea ice deformation state from synthetic aperture radar imagery - part I: comparison of C- and L-band and different polarizations. -IEEE Transact. Geosci. Remote Sensing 45(11): 3610-3622, doi:10.1109/TGRS.2007.903711.

Dierking, W. & Dall, J. (2008): Sea ice deformation state from synthetic aperture radar imagery part II: effects of spatial resolution and noise level.- IEEE Transact. Geosci. Remote Sensing 46(8): 2197-2207, doi:10.1109/TGRS.2008.917267.

Dierking, W., Pettersson, M. & Askne, J. (1999): Multifrequency scatterometer measurements of Baltic Sea ice during EMAC-95.- Internat. J. Remote Sensing 20: 349-372.

Eicken, H. (1994): Structure of under-ice melt ponds in the central Arctic and their effect on the sea-ice cover.- Limnol. Oceanogr. 39(3): 682-694.

Eicken, H., Lensu, M., Leppäranta, M., Tuckeriii, W., Gow, A. & Salmela, O. (1995): Thickness, structure, and properties of level summer multiyear ice in the Eurasian sector of the Arctic Ocean.- J. Geophys Res. 100(C11): 22697-22710.

ESA (2006): ESA Living Planet Scientific Challenges.- ESA-SP-1304.

Fetterer, F. M., Gineris, D. & Kwok, R. (1994): Sea ice type maps from Alaska synthetic aperture radar facility imagery: an assessment.- J. Geophys. Res. 99(C11): 22443-22458.

Frolov, I., Gudkovich, Z.M., Radionov, V.F., Shirochkov, A.V. & Timokhov, L.A. (2005): The Arctic Basin – results from the Russian drifting stations. - Springer Verlag, Berlin, Heidelberg, 1-272.

Fütterer, D.K. (ed) (1992): Arctic'91: The Expedition ARK-VIII/3 of RV "Polarstern" in 1991.- Reports Polar Res. 107: 1 267.

Garbrecht, T., Lüpkes, C., Augstein, E. & Wamser, C. (1999): The influence of a sea ice ridge on the low-level air flow.- J. Geophys. Res. 104(D20): 24499-24507.

Garbrecht, T., Lüpkes, C., Hartmann, J. & Wolff, M. (2002): Atmospheric drag coefficients over sea ice – validation of a parameterisation concept.- Tellus 54A: 205-219.

Giles, K.A., Laxon, S.W. & Ridout, A.L. (2008): Circumpolar thinning of Arctic sea ice following the 2007 record ice extent minimum.- Geophys. Res. Lett. 35: L22502, doi:10.1029/2008GL035710.

Haas, C. (1997): Sea-ice thickness measurements using seismic and electromagnetic-inductive techniques.- PhD thesis Univ. Bremen, Rep. Polar Res. 223, 1-161.

Haas, C. (1998): Evaluation of ship-based electromagnetic-inductive thickness measurements of summer sea-ice in the Bellingshausen and Amundsen Seas, Antarctica.- Cold Regions Sci. Technol. 27: 1-16.

Haas, C. (2004): Late-summer sea ice thickness variability in the Arctic Transpolar Drift 1991-2001 derived from ground-based electromagnetic sounding.- Geophys. Res. Lett. 31, L09402, doi:10.1029/2003GL019394

Haas, C. & Eicken, H. (2001): Interannual variability of summer sea ice thickness in the Siberian and central Arctic under different atmospheric circulation regimes.- J. Geophys. Res. 106(C3): 4449-4462, doi:10.1029/1999JC000088.

Haas, C., Gerland, S., Eicken, H. & Miller, H. (1997): Comparison of sea-ice thickness measurements under summer and winter conditions in the Arctic using a small electromagnetic induction device.- Geophys. 62: 749-757.

Haas, C., Hendricks, S., Eicken, H. & Herber, A. (2010): Synoptic airborne thickness surveys reveal state of Arctic sea ice cover.- Geophys. Res. Lett. 37, L09501, doi:10.1029/2010GL042652.

Haas, C., Liu, Q. & Martin, T. (1999): Retrieval of Antarctic sea-ice pressure ridge frequencies from ERS SAR imagery by means of in-situ laser profiling and usage of a neural network.- Internat. J. Remote Sensing 20(15): 3111-3123 .

Haas, C., Pfaffling, A., Hendricks, S., Rabenstein, L., Etienne, J.-L. & Rigor, I. (2008): Reduced ice thickness in Arctic Transpolar Drift favours rapid ice retreat.- Geophys. Res. Lett., 35, L17501, doi:10.1029/ 2008GL034457.

Hvidegaard, S.M. & Forsberg, R. (2002): Sea-ice thickness from airborne laser altimetry over the Arctic Ocean north of Greenland.- Geophys. Res. Lett. 29(20), 1952, doi:10.1029/2001GL014474.

IGOS (2007): Integrated Global Observing Strategy (IGOS).- Cryosphere Theme Rep., August 2007, WMO/TD-No. 1405. http://igos-cryosphere.org/

Kaleschke, L., Tian-Kunze, X., Maaß, N., Mäkynen, M. & Drusch, M. (2012): Sea ice thickness retrieval from SMOS brightness temperatures during the Arctic freeze-up period.- Geophys. Res. Lett. doi: 10.1029/2012GL050916.

Kay, J.E., Holland, M.M. & Jahn, A. (2011): Inter-annual to multi-decadal Arctic sea ice extent trends in a warming world.- Geophys. Res. Let. 38, L15708, doi: 10.1029/2011GL048008.

Koerner, R.M. (1973): The mass balance of the sea ice of the Arctic Ocean. - J. Glaciol. 12: 173-185.

Kwok, R., Cunningham, G.F. & Nghiem, S.V. (2003): A study of the onset of melt over the Arctic Ocean in RADARSAT synthetic aperture radar data.- J. Geophys. Res. 108(C11), 3363, doi: 10.1029/2002JC001363, 2003

Kwok, R., Cunningham, G.F., Wensnahan, M., Rigor, I., Zwally, H.J. & Yi, D. (2009): Thinning and volume loss of the Arctic Ocean sea ice cover: 2003-2008.- J. Geophys. Res. 114:C07005.

Kwok, R., Cunningham, G.F., Manizade S.S. & Krabill, W.B. (2012): Arctic sea ice freeboard from IceBridge acquisitions in 2009: estimates and comparisons with ICESat.- J. Geophys. Res. 117, C02018, doi: 10.1029/2011JC007654.

Laxon, S., Peacock, N. & Smith, D. (2003): High interannual variability of sea ice thickness in the Arctic region.- Nature 425: 947-950.

Lemke, P., Ren, J., Alley, R., Allison, I., Carrasco, J., Flato, G., Fujii, Y., Kaser, G., Mote, P., Thomas, R. & Zhang, T. (2007): Observations: changes in snow, ice and frozen ground.- In: Climate Change 2007: The Physical Science Basis. Contrib. WG I to the Fourth Assessm. Rep. IPCC. Cambridge Univ. Press, Cambridge, UK and New York, NY, USA.

Lubin, D. & Massom, R. (2006): Polar Remote Sensing, Vol. I: Atmosphere and Oceans. Springer Praxis, Chichester, UK, 1-756.

Markus, T., Stroeve, J.C. & Miller, J. (2009): Recent changes in Arctic sea ice melt onset, freeze-up, and melt season length.- J. Geophys. Res. 114, C12024, doi: 10.1029/2009JC005436.

Maslanik, J., Stroeve, J., Fowler, C. & Emery, W. (2011): Distribution and trends in Arctic sea ice age through spring 2011.- Geophys. Res. Lett. 38, L13502, doi:10.1029/2011GL047735.

Nakamura, K., Wakabayashi, H., Uto, S., Naoik, K., Nishio, F. & Uratsuka, S. (2006): Sea ice thickness retrieval in the Sea of Okhotsk using dual-polarization data.- Annals Glaciol. 44: 261-268.

Nakamura, K., Wakabayashi, H., Uto, S., Ushio, S. & Nishio, F. (2009): Observation of sea ice thickness using ENVISAT data from Lützow-Holm Bay, East-Antarctica.- IEEE Geosci. Remote Sensing Lett. 6(2): 277-281.

Nansen, F. (1897): Farthest North, 2 vols., New York, Harper, 1897. (Fram over Polhavet: Den norske polarfaerd, 1893-1896. 2 vols. Oslo, Aschehoug, 1897.)

Perovich, D.K., Grenfell, T.C., Light, B., Elder, B.C., Harbeck, J., Polashenski, C., Tucker III, W.B., & Stelmach, C. (2009): Transpolar observations of the morphological properties of Arctic sea ice.- J. Geophys. Res. 114, C00A04, doi:10.1029/ 2008JC004892.

Prinsenberg, S., Holladay, S. & Lee, J. (2002): Measuring ice thickness with EISFlow™, a fixed-mounted helicopter electromagnetic laser system.- Proceed. Twelfth Internat. Offshore and Polar Engineering Conference, Kitakyushu, Japan, May 26-31: 737-740.

Romanov, I.P. (1995): Atlas of Ice and Snow of the Arctic Basin and Siberian Shelf Seas. - Dr. Alfred Tunik, translator and editor. Second edition of atlas and monograph. Revised and expanded. ISBN 0-9644311-3-0. Backbone Publishing Company.

Steffen, K. & Heinrichs, J. (1994): Feasibility of sea ice typing with synthetic aperture radar (SAR): merging of Landsat thematic mapper and ERS-1 SAR satellite imagery.- J. Geophys. Res. 99(C11): 22 413-22 424.

Stroeve, J., Sereze, M., Drobot, S., Gearheard, S., Holland, M., .Maslanik, J., Meier, W. & Scambos, T. (2008): Arctic sea ice extent plummets in 2007.- Eos Trans. AGU 89(2).

Tucker III, W.B., Gow, A.J., Meese, D.A., Bosworth, H.W. & Reimnitz, E. (1999): Physical characteristics of summer sea ice across the Arctic Ocean.- J. Geophys. Res. 104(C1): 1489-1504, doi: 10.1029/98JC02607.

Turner, J., Comiso, J.C., Marshall, G.J., Lachlan-Cope, T.A., Bracegirdle, T., Maksym, T., Meredith, M.P., Wang, Z. & Orr, A. (2009): Non-annular atmospheric circulation change induced by stratospheric ozone depletion and its role in the recent increase of Antarctic sea ice extent. - Geophys. Res. Lett. 36, L08502, doi: 10.1029/2009GL037524.

Ulander, L.M.H., Carlström, A. & Askne, J. (1995): Effect of frost flowers, rough saline snow and slush on the ERS-1 backscatter of thin arctic sea ice. - Internat. J. Remote Sensing 16(17): 3287-3305.

Untersteiner, N, Thorndike, A.S., Rothrock, D.A. & Hunkins, K.L. (2007): AIDJEX revisited: a look back at the U.S.-Canadian Arctic Ice Dynamics Joint Experiment 1970-78.- Arctic 60(3): 327-336.

Viehoff, T. (1990): A shipborne AVHRR-HRPT receiving and image processsing system for polar research.- Internat. J Remote Sensing 11(5): 877-886 .

Wadhams, P. (2000): Ice in the ocean.- Gordon & Breach Science Publishers, Singapore, 1-351.

Wang, M. & Overland, J.E. (2009): A sea-ice free summer Arctic within 30 years?- Geophys. Res. Lett. 36, L07502, doi: 10.1029/2009GL037820.

Winebrenner, D.P., Holt, B. & Nelson, E.D. (1996): Observation of autumn freeze-up in the Beaufort and Chukchi Seas using the ERS-1 synthetic aperture radar.- J. Geophys. Res. 101(C7): 16 401-16419.

Winebrenner, D.P., Nelson, E.D., Colony, R. &West, R.D. (1994): Observation of melt onset on multiyear arctic sea ice using the ERS-1 synthetic aperture radar.- J. Geophys. Res. 99(C11): 22 425-22 441.

Wingham, D.J., Francis, C.R., Baker, S., Bouzinac, C., Brockley, D., Cullen, R., de Chateau-Thierry, P., Laxon, S.W., Mallow, U., Mavrocordatos, C., Phalippou, L., Ratier, G., Rey, L., Rostan, F., Viau, P. & Wallis, D.W. (2006): Cryosat: a mission to determine the fluctuations in the Earth's land and marine ice fields.- Advances Space Res. 37: 841-871.